SPECIATION OF RUTHENIUM-BASED CANDIDATE DRUGS FOR CANCER TREATMENT AND COPPER AS A POTENTIAL BIOMARKER FOR CANCER DIAGNOSIS IN HUMAN SERUM

Katarina Marković

Doctoral Dissertation
Jožef Stefan International Postgraduate School
Ljubljana, Slovenia

Supervisor: Prof. Dr. Radmila Milačič, Jožef Stefan Institute, Jamova 39, 1000 Ljubljana, Slovenia

Evaluation Board:
Prof. Dr. Maja Ponikvar-Svet, Chair, Jožef Stefan Institute, Jamova 39, 1000 Ljubljana, Slovenia
Prof. Dr. Maja Čemažar, Member, Institute of Oncology, Zaloška 2, 1000 Ljubljana, Slovenia
Prof. Dr. Dirk Schaumlöffel, Member, Institute of Analytical Sciences and Physico-Chemistry for the Environment and Materials, Technopôle Helioparc 2 avenue P. Angot 64053 Pau Cedex 9, France

MEDNARODNA PODIPLOMSKA ŠOLA JOŽEFA STEFANA
JOŽEF STEFAN INTERNATIONAL POSTGRADUATE SCHOOL

Katarina Marković

SPECIATION OF RUTHENIUM-BASED CANDIDATE DRUGS FOR CANCER TREATMENT AND COPPER AS A POTENTIAL BIOMARKER FOR CANCER DIAGNOSIS IN HUMAN SERUM

Doctoral Dissertation

SPECIACIJA RUTENIJEVIH SPOJIN ZA ZDRAVLJENJE RAKA IN BAKRA KOT MOŽNEGA BIOMARKERJA PRI DIAGNOSTIKI RAKA V HUMANEM SERUMU

Doktorska disertacija

Supervisor: Prof. Dr. Radmila Milačič

Ljubljana, Slovenia, August 2022

To my family. Thank you.

Acknowledgments

This PhD thesis was completed at the Department of Environmental Sciences at the Jožef Stefan Institute. First, I would like to thank my dissertation supervisor Prof. Dr. Radmila Milačič for her outstanding support, help and guidance during my studies. Together with Prof. Dr. Janez Ščančar, they gave me the opportunity to work and grow as a scientist in their laboratory. They were always available for discussions and scientific advice on my research. Without their help and endless support, this study would not have been possible. I am also grateful for the financial support of the Slovenian Research Agency (Program group P1-0143) and for the Junior Researcher Grant (52052).

I would like to thank the evaluation board members Prof. Dr. Maja Ponikvar-Svet, Prof. Dr. Maja Čemažar and Prof. Dr. Dirk Schaumlöffel for reviewing the manuscript and evaluating my work in the doctoral dissertation.

I want to express gratitude to my dear co-workers Stefan, Janja, Tea, Tjaša, Majda, Mišel, Belma, Martina, Lucija and Matic for being great company during long laboratory hours and for all their help when needed. I would also like to thank other colleagues from JSI and TU WIEN for our pleasant time together during this journey.

Lastly, I would like to thank my loved ones for being supportive. None of this would have been possible if you had not stood by my side.

Abstract

According to the World Health Organization (WHO), cancer represents the second leading cause of mortality, with almost 10 million deaths in 2020. A broad spectra of cancer treatments are being developed, among them are metal-based drugs. Consistent with the available data, platinum (Pt)-based chemotherapeutics are still widely used to treat various cancers. The main drawback of Pt-based chemotherapeutics is their high toxicity, which leads to severe side effects. So, this research is oriented towards the development of new anticancer drugs. Two of the promising drug candidates are Ru (II) and Ru (III) complexes. An important step in a candidate drug's characterization is the pharmacological evaluation of its interactions with serum proteins. It provides data for the elucidation of the mechanism of antitumor therapy, the behaviour of the intact drug, its biotransformation in clinical samples at physiologically relevant concentrations and, as the final goal, its dosage adjustment. In investigations of the performance of new candidate drugs, it is also important to elucidate the kinetics of drug bindings to human serum proteins. A speciation analysis can largely acquire this information. Two ruthenium (Ru) complexes, i.e., [(η6-p-cymene)Ru(1-hydroxypyridine-2(1H)-thionato)Cl] **(1)** and [(η6-p-cymene)Ru(1-hydroxypyridine-2(1H)-thionato)pta]PF6 **(2)** (where pta = 1,3,5-triaza-7-phosphaadamantane), were studied. Conjoint liquid chromatography (CLC) monolithic column, assembling convective interaction media (CIM) protein G and diethylaminoethyl (DEAE) disks, was used for the separation of unbound Ru species from those bound to human serum transferrin (Tf), albumin (HSA) and immunoglobulins G (IgG). Eluted proteins were monitored by UV spectrometry at 278 nm, while Ru species were quantified by post-column isotope dilution inductively coupled plasma mass spectrometry (ID-ICP-MS). The binding kinetics of chlorido **(1)** and pta complex **(2)** to serum proteins was followed from 5 min to 48 h after incubation with human serum. Speciation analysis data revealed that the interaction with serum proteins was faster and more extensive in the chlorido **(1)** complex.

Ceruloplasmin (Cp) is human plasma's major copper-carrying (Cu) protein. Due to copper's important physiological functions and its role in various diseases, it is necessary to quantify the concentration bound to Cp and the exchangeable form of Cu. In the present work, CLC on short-bed CIM monolithic disks was used to separate the Cu bound to low molecular mass (LMM) species and the Cu bound to Cp and HSA in human serum. Two immunoaffinity CIMmic albumin depletion (α -HSA) disks and one CIMmic weak anion-exchange DEAE disk were assembled in a single housing, forming a CLC monolithic column. The separated Cu species were quantified by post-column ID-ICP-MS, while the elution profile of the proteins was followed by UV detection at 278 nm. This novel developed method was successfully applied in the determination of Cu-Cp, Cu-HSA and a fraction that most probably corresponds to the Cu-LMM species in the human serum of healthy individuals, transplanted renal patients and cancer patients. The data from the present research provide an important new analytical tool that can be used to assess Cu metabolic disorders in many diseases.

Povzetek

Po podatkih Svetovne zdravstvene organizacije (WHO) je rak drugi najpogostejši vzrok umrljivosti. V letu 2020 je za rakom umrlo skoraj 10 milijonov ljudi. Med različnimi načini zdravljenja raka se uporabljajo tudi zdravila na osnovi kovin. Med njimi še vedno pogosto uporabljajo kemoterapevtike na osnovi platine (Pt). Njihova glavna pomanjkljivost je visoka toksičnost, ki vodi do resnih stranskih učinkov zdravila. Zaradi omenjenega dejstva so raziskave usmerjene v razvoj novih zdravil proti raku. Eni od obetavnih kandidatov so Ru(II) in Ru(III) kompleksi. Pomemben korak pri karakterizaciji zdravila je farmakološka ocena njegovih interakcij s serumskimi proteini, ki omogoča pridobivanje podatkov za poznavanje mehanizmov protitumorske terapije, obnašanja zdravila, njegove biotransformacije v kliničnih vzorcih pri fiziološko pomembnih koncentracijah in kot končni cilj prilagoditve njegovega odmerjanja. Pri raziskavah učinkovitosti novih potencialnih zdravil za zdravljenje raka je pomembno poznati kinetiko vezave zdravila na serumske proteine. Te informacije lahko v veliki meri pridobimo s speciacijsko analizo. Preučevali smo dva kompleksa rutenija (Ru), in sicer [(η6-p-cimen)Ru(1-hidroksipiridin-2(1H)-tionato)Cl] (1) ter [(η6-p-cimen)Ru(1-hidroksipiridin-2 (1H)-tionato)pta]PF6 (2) (kjer je pta = 1,3,5-triaza-7-fosfaadamantan). Za ločevanje nevezanih zvrsti Ru od tistih, ki so vezane na humani serumski transferin (Tf), albumin (HSA) in imunoglobulin G (IgG), smo uporabili združeno monolitno kolono (CLC), sestavljeno iz diskov s konvektivnim prenosom snovi (CIM), tako da smo v kromatografski sklop združili protein G in dietilaminoetil (DEAE) diska. Elucijo proteinov smo spremljali z UV spektrometrijo (278 nm), medtem ko smo kemijske zvrsti Ru kvantificirali s tehniko pokolonskega izotopskega redčenja v masni spektrometriji z induktivno sklopljeno plazmo (ID-ICP-MS). Kinetiko vezave klorido (1) in pta kompleksa (2) na serumske proteine smo spremljali 5 minut do 48 ur po inkubaciji človeškega seruma z omenjenima spojinama. Rezultati so pokazali, da je bila interakcija s serumskimi proteini hitrejša in obsežnejša pri klorido (1) kompleksu.

Ceruloplazmin (Cp) je glavni protein, ki prenaša baker (Cu) v človeški plazmi. Zaradi pomembnih fizioloških funkcij Cu in njegove vloge pri različnih boleznih je potrebno kvantificirati koncentracijo Cu, vezanega na Cp, in izmenljivo obliko Cu. V predstavljeni raziskavi smo uporabili CLC na kratkih CIM monolitnih diskih za ločevanje Cu v človeškem serumu, vezanega na kemijske zvrsti z nizko molekulsko maso (LMM), ter Cu, vezanega na Cp in HSA. Dva imunoafinitetna CIMmic diska za vezavo albumina (α-HSA) in en šibek anionsko izmenjalen CIMmic DEAE disk smo vstavili v ohišje CLC kolone. Ločene kemijske zvrsti Cu smo kvantificirali s tehniko pokolonskega izotopskega redčenja ID-ICP-MS, medtem ko smo elucijskemu profilu proteinov sledili z UV detekcijo pri 278 nm. Novo analizno metodo smo uspešno uporabili pri določanju Cu-Cp, Cu-HSA in frakcije, ki najverjetneje ustreza Cu-LMM v človeškem serumu. Analizirali smo serum zdravih oseb, bolnikov s presajeno ledvico in rakavih bolnikov. Predstavljena raziskava pomembno prispeva k novim analiznim tehnikam, ki jih lahko uporabimo za oceno presnovnih motenj Cu pri številnih boleznih.

Contents

List of Figures

List of Tables

Abbreviations

Al	.....	aluminium
AcOH	.....	acetic acid
Ar	.....	argon
CIM	.....	convective interaction media
CLC	.....	conjoined liquid chromatography
CPS	.....	counts per second
Cr	.....	chromium
CE	.....	capillary electrophoresis
Cu	.....	copper
Cp	.....	ceruloplasmin
DEAE	.....	diethylaminoethyl
ESI	.....	electrospray ionization
FPLC	.....	fast protein liquid chromatography
GC	.....	gas chromatography
GE	.....	gas chromatography
He	.....	helium
HMM	.....	High molecular mass
HPLC	.....	high performance liquid chromatography
HSA	.....	human serum albumin
IE	.....	ion exchange chromatography
ICP-MS	.....	inductively coupled plasma – mass spectrometry
ID	.....	isotope dilution
IDMS	.....	isotope dilution – mass spectrometry
IgG	.....	immunoglobulin G
Rh	.....	rhodium
LOD	.....	limit of detection
LOQ	.....	limit of quantification
m/z	.....	mass/charge
MALDI	.....	matrix-assisted laser desorption ionization
MOPS	.....	3-morpholinopropane-1-sulfonic acid
LC	.....	liquid chromatography
LMM	.....	low molecular mass
Pt	.....	platinum
Ru	.....	ruthenium
RP	.....	reversed phase
RSD	.....	relative standard deviation
s.p.	.....	supra pure
SEC	.....	size exclusion chromatography
Tf	.....	transferrin
Tris	.....	tris(hydroxymethyl)aminomethane
UV	.....	ultraviolet

WHO ..... World Health Organization
IUPAC ..... International Union of Pure and Applied Chemistry
(1) ..... [(η 6-p-cymene)Ru(1-hydroxypyridine-2(1H)-thionato)Cl]
(2) ..... [(η 6-p-cimen)Ru(1-hidroksipiridin-2 (1H)-tionato)pta]PF6

Chapter 1

Introduction

1.1 Speciation Analysis

Speciation analysis is, according to the International Union of Pure and Applied Chemistry (IUPAC), the set of analytical activities used for the identification and/or quantification of different chemical species (one or more) present in the sample [1]. In the last three decades, the rising awareness of the direct relationship between the toxicity effects of elements (especially metals) and their chemical species has led to the need for speciation analysis. Thus, speciation analysis has proved to be an indispensable tool in agriculture, pharmacy, biomedical sciences, and the environmental and food industries, where measuring only the total element concentration is insufficient. Identifying the different chemical species and measuring their concentrations enables a better understanding and detailed evaluation of the possible risks, since it determines the element mobility, solubility, toxicity, bioavailability, bioaccumulation and metabolic pathways [2]. One of the examples of species toxicity can be seen in chromium (Cr), the properties of which primarily depend on its oxidation state. Cr(III) was assumed to be an essential micronutrient for mammals [3], while Cr(VI) is a well-known human carcinogen [4]. Data acquired by speciation analysis can significantly contribute to the field of metallomics, which targets an understanding of the molecular mechanisms of metal-dependent life processes [5]. Therefore, speciation analysis is undoubtedly needed in evaluating a human health risk assessment, the quality control of various products and environmental pollution monitoring [6].

1.1.1 Importance of speciation analysis in human serum samples

The serum is the blood constituent free from cells and proteins (fibrinogen) that forms the clot. It is in a supernatant fraction obtained by centrifugation after whole blood clotting. It is an aqueous solution (around 95% is water) that contains all other circulating proteins that are not involved in blood clotting, electrolytes, nutrients (carbohydrates, lipids and amino acids), hormones and other exogenous substances (e.g., drugs) present in the body. It is essential in regulating the pH and ion composition in extracellular fluid and the body temperature. Since the blood is in contact with all the tissues and organs in the organism, it is deployed as the main discharge pathway for all the excrements produced by metabolism [7]. So, any significant deviation in the normal physiological functioning can alter human blood's chemical or protein composition and, consequently, human plasma. Thus, blood and serum represent the main media for numerous diagnostic tests in routine clinical analysis [8]. In addition, human serum can be used in many applications, such as the growth factor for cultured cells and leukocyte antigen typing to screen human donors'

compatibility and determine a therapeutic index of drug candidates. Since the drug's efficacy depends on the distribution and targeted transportation to the treatment site, it is crucial to study the behaviour of an intact drug in human serum [9]. This is especially significant when designing and characterising new metal-based candidates' chemotherapeutics, since their side effects are usually highly expressed. Therefore, the study of drug biotransformation after injection and the drug's interactions with serum proteins at physiologically relevant concentrations is needed to elucidate the mechanism of anticancer therapy and, finally, the dosage adjustment [10]. This information can be largely obtained by speciation analysis [9]–[14].

The present thesis used speciation analysis to study the kinetics of ruthenium (Ru)-based candidate drugs with serum proteins and investigate the distribution of the intact Ru drug and its species bound to serum proteins. Two Ru-based complexes, [(η 6-p-cymene)Ru(1-hydroxypyridine-2(1H)-thionato)Cl] (1) and [(η 6-p-cymene)Ru(1-hydroxypyridine-2(1H)-thionato)pta]PF6 (2) (where pta = 1,3,5-triaza-7-phosphaadamantane), were selected [15]. The obtained knowledge contributes to the candidate drug's characterization and provides data for the elucidation of the toxicity mechanisms.

A speciation analyses of human serum can also be applied in clinical practice, where the existing clinical methods are not selective enough. In the second part of the thesis, a novel analytical method was developed to study copper (Cu) species in human serum, i.e., Cu bound to ceruloplasmin (Cp), human serum albumin (HSA) and amino acids. A speciation analysis was shown to be a more reliable technique for such studies than routine clinical tests based on the immunological method [16].

1.1.2 Analytical tools for a speciation analysis of human serum samples

With a growing understanding of the importance of a reliable determination of chemical species present in the sample, there was a need to develop reliable analytical methods for a speciation analysis. Such an analysis imposes additional challenges regarding the sample preparation and measurement. The critical step in a speciation analysis is related to preserving the species' integrity through all the steps of the analytical procedure, from sampling, sample preparation and speciation analysis. The big challenge is also to achieve an effective separation of the targeted species in the sample analysed and their sensitive determination. Elemental speciation analysis was improved with the development of instrumentation due to the lower limits of detection (LOD), which enabled the switch from measuring the total trace elements concentration to the quantification of each species present in the sample [17]. For the separation of species present in serum samples, various chromatographic techniques, e.g., liquid (LC) and gas chromatography (GC) as well as capillary (CE) and gel (GE) electrophoresis [18]–[21], while for the detection of the separated species, element-specific detectors like fluorescence, emission, and absorption spectroscopy, and mass spectrometry-based techniques (inductively coupled plasma mass spectrometry, ICP-MS) are frequently used [22]. Identification of the separated species is most commonly obtained by mass spectrometry techniques such as electrospray ionization (ESI) and matrix-assisted laser desorption/ionization (MALDI)[23]–[25].

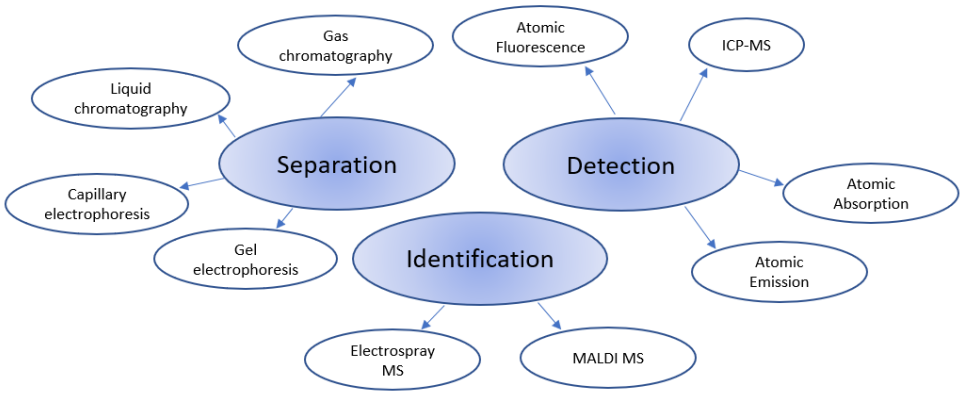

Figure 1: Hyphenated techniques for speciation analysis, adopted from [26].

1.1.3 High-performance liquid chromatography for a speciation analysis of metal-based species in human serum samples

For a reliable speciation analysis in human serum and to study the distribution of the individual metal species, an efficient separation of the metal ions and their complexes is needed. As the most common analytical tool for separating different chemical species present in the serum sample, high-performance liquid chromatography (HPLC) is applied. The flexibility of HPLC allows various types of chromatographic columns to be used, which, together with its compatibility with different detectors, enables the broadening of the spectra of analysed substances [19]. Such coupling evolved into the development of hyphenated techniques, which became methods of choice for speciation analysis. The most studied metal-based species are metal-amino acid, metal-protein, metal-low molecular mass (LMM) organic acid complexes and metal-based drugs and their species in serum samples. For the speciation studies of platinum (Pt)-based chemotherapeutics and their metabolites in wastewater and urine samples, reversed-phase (C18) and hydrophilic interaction chromatography (HILIC) columns were used [27]–[30], while in speciation studies of cancer metallodrugs and the metalloprotein distribution in human serum and the studies of the serum binding properties, ion exchange (IE) columns, both strong and weak, could be used [31]–[34]. Size exclusion chromatography (SEC) is also frequently applied in speciation analysis [35], [36]. It can be combined with other chromatographic columns to expand the variety of analysed species. Species separated based on SEC are further submitted to two-dimensional chromatographic separation, using fast protein liquid chromatography (FPLC), IE or immunoaffinity columns [32], [37], [38]. SEC was also combined with monolithic columns, where the study of the distribution of cisplatin in human serum was performed. First, rapid Pt fractionation was performed by SEC on a HiTrap desalting column, where the proteins (high molecular weight fraction, HMM) were separated from unbound (LMM) Pt species. Afterwards, the protein peak was collected and injected onto the IE monolithic column, which enables the separation of the Pt species bound to human serum proteins [32]. Nonetheless, SEC has some serious limitations [39]:

- Broadening of the target protein peak due highly viscous sample or too high flow rates
- Irreversible precipitation of the protein, which prevents a quantitative elution from the stationary phase of the column
- The low resolution of the SEC column disables the selective separation of proteins

- Moderately long chromatographic runs (typically up to 60 min) impair kinetic studies

1.2 Monolithic Supports

Since 1990 monolithic supports have received increasing attention as an alternative to the commonly used particle-packed chromatographic columns [40]–[43]. They are suitable for numerous applications, such as separating large biomolecules, i.e., virus particles, vesicles, proteins, RNAs, plasmids and other forms of DNA. Monolithic chromatography has several advantages over particle-packed columns. Among them is the column's low back pressure, enabling higher flow rates and sample throughput. Convective mass transport allows for fast and efficient chromatographic separations and thus, shortening the chromatographic run time. The resolution and capacity of monoliths showed flow-independency [44]. Generally, monoliths have much greater porosity and mass permeability than particle-packed columns to sustain a greater number of analysed samples and more rigorous cleaning. Since the monoliths are single, coherent and rigid units, they do not have a void volume. Monoliths are classified as silica-based and polymer-based (methacrylate and poly(styrene-co-divinylbenzene)) supports and can be prepared in different shapes and sizes (disks, columns and tube forms). The copolymerization with different functional groups allows the formation of monolithic columns with various chromatographic separation modes (RP, IE, hydrophobic interaction and affinity chromatography). An additional advantage of the monolithic columns is the ability to combine different column disks with a different mode of operation into a single housing, forming a so-called conjoined liquid chromatography (CLC) column, which enables two-dimensional separation (2D) to be carried out in a single chromatographic run [40], [45].

The application of monolithic chromatography is broad for industrial and commercial downstream processing and research purposes. Lately, convective interaction media (CIM) monoliths have been applied for the purification of gene therapy vectors (adenoviruses, lentiviruses, adeno-associated viruses, retroviruses and pDNA) used in vaccine production [46], [47]. Moreover, monoliths are successfully used in the field of elemental speciation analysis in environmental [48]–[50], food [51]–[53] and biological samples [54], [55].

1.2.1 Monolithic supports for a speciation analysis of metal-based species in human serum samples

Due to the above-listed advantages, CIM poly-methacrylate-based monolithic supports are increasingly used in speciation analysis. They enable species integrity during chromatographic separation and thus prevent species interconversions. Preserving species integrity in the analysis of labile metal complexes is essential for their reliable determinations. For example, in our group, aluminium (Al) speciation was performed using a weak anion-exchange CIM DEAE fast-monolithic disk hyphenated to ICP-MS for the speciation of HMM Al species in human serum at physiological concentrations [56]. Furthermore, four weak anion-exchange CIM DEAE disks were placed into a single housing, forming a CIM DEAE monolithic column, which was used in a kinetics study of the interaction of Cr(III) and Cr(VI) species with serum proteins at physiologically relevant concentrations [57]. The rigorous cleaning of the DEAE supports (rinsing with 1 M NaOH) lowers the blanks, making anion exchange monoliths superior to the particle-packed columns for analysing the concentrations of trace metal species in biological samples. In addition, the CIM DEAE and immunoaffinity affinity CIM Protein G disks were assembled into a single housing, forming a CLC monolithic column that makes it possible to perform

a 2D separation mode in one chromatographic run. Such a CLC monolithic column was used to study the speciation and kinetics of metal-based chemotherapeutics in human serum samples. Intact Pt-based drugs were separated from their individual bio-transformed species bound to serum proteins. On the first disk (Protein G), the fraction of the Pt-drug bound to the IgG was retained, while the intact Pt-drug, Pt bound to transferrin (Tf) and human serum albumin (HSA) were separated on the second CIM DEAE disk. Afterwards, the fraction of Pt-IgG was eluted. All the separated serum proteins were detected online by UV detection at 278 nm, while the eluted Pt species were accurately quantified by the post-column ID-ICP-MS technique [31], [58]. The same methodology was also applied in the study of selected Ru-based chemotherapeutics [59].

1.3 Cancer

Cancer represents a large group of frequently occurring diseases characterised by uncontrolled cell growth (proliferation) with the potential to spread to the surrounding normal tissues, enter the circulation or lymphatic system, and spread throughout the body (metastasis). More than 100 types of cancer can affect any organ or tissue in the body. According to the World Health Organisation (WHO), cancer represents the second leading cause of mortality, leading to almost 10 million deaths in 2020 [60] and 19.3 million new cases worldwide. There are estimations that the global cancer burden will be 28.4 million cases in 2040, with a 47% rise from 2020. There is also a prediction that transitioning will meet a higher increase rate (64 to 95%) in comparison to the transitioned (32 to 56%) countries [61]. In countries of the European Union, estimates show 4 million new cases and 1.9 million deaths in 2020. The most frequent cancers in 2020 were: breast in woman (530 000), colorectum (520 000), lung (480 000) and prostate (470 000), while the most common causes of death in 2020 were: lung (380 000), colorectal (250 000), breast (140 000) and pancreatic (130 000) cancers [62].

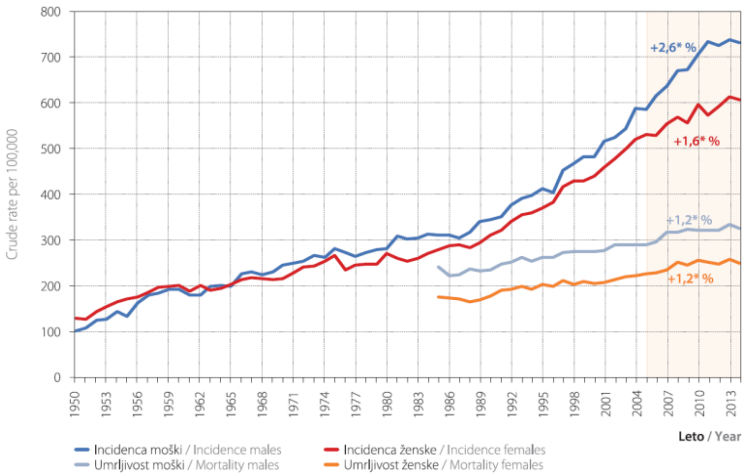

Figure 2: Cancer incidence and mortality for males and females in Slovenia 1950-2014 (Reproduced from freely available at Cancer registry, slora.si).

The incidence of cancer cases has significantly increased in the past decades due to the expanded human lifespan and population growth. The main cancer-inducing factors (carcinogens) are divided into three groups: external, exposure and infections. External factors are tobacco smoking, moderate or heavy alcohol consumption, poor dietary habits, which are influenced mainly by obesity (responsible for up to 20% of cancer death in the

developed world), low fruit and vegetable intake and physical inactivity. Carcinogens related to exposure encompass ionizing and solar (ultraviolet) radiation, environmental pollution (especially air) and occupational exposure to different chemicals. Other risk factors include hereditary cancers that encompass 5-10% and infections, which are responsible for 16% of the total incidence rate. Viral infections such as human papillomavirus (HPV), hepatitis B and C virus, Epstein-Barr virus and human immunodeficiency virus (HIV) can potentially lead to the development of cancer [63]. Bacterial and parasitic infections can also represent the risk factors for cancer, especially *Helicobacter pylori* and *Schistosomiasis haematobium* [64]. Cancer cells differ from normal cells in several ways. They mostly show abnormalities in the mechanisms related to cell proliferation, differentiation and death. Cancer cells acquire mechanisms to sustain proliferative signalling. Another difference between cancer and normal cells is that proliferation of cancer cells is not responsive to density-dependent inhibition, meaning that the reach of finite cell density depends on the availability of growth factors. Contrary, normal cells divide in culture until they reach fixed cell density [65].

Cancer cells also exhibit reduced requirements for extracellular polypeptide growth factors. In some cases, cancer cells can produce growth factors leading to constant auto-stimulation of proliferation. Growth factors can also promote the formation of new blood vessels, providing the cancer cells with oxygen and nutrients, and facilitating metastatic processes [66]. In addition, cancer cells are also less adhesive than normal cells, resulting in an increased ability to metastasize to the surrounding tissue. Another important characteristic of cancer cells is the failure of normal differentiation, which is triggered by proliferation [67]. All these carcinogenesis (cancer formation) mechanisms have been extensively studied to prevent cancer formation and establish appropriate and effective therapy [68].

1.3.1 Chemotherapy

The selection of cancer treatment is based on the type of cancer and its stage. The majority of cases require a combination of different treatments. The most common treatments for localized tumour tissue are surgery and radiation therapy, while drug treatments such as chemotherapy, immunotherapy and target therapy affect the complete organism [69]. Chemotherapeutics are commonly used to treat a spreading cancer due to their non-local reactivity to uncontrolled proliferation. The characteristics of chemotherapeutics, such as non-specificity towards cancer cells, are simultaneously affecting normal cells, provoking severe side effects, such as neurotoxicity, nephrotoxicity, infertility, teratogenicity and alopecia [70]. The greatest issue and medical challenge of chemotherapy treatment is the development of drug resistance, which is the first cause of cancer-associated death.

Chemotherapeutic drugs are classified according to the reaction mechanism: alkylating agents which react with nucleophilic centres of proteins and nucleic acids, inactivating DNA replication and transcription (nitrogen mustards, nitrosoureas, and alkyl sulfonates), while the Pt-based chemotherapeutics exhibit a similar mechanism of action, but are not alkylating agents; antimetabolites which inhibit DNA replication (cytidine analogues, folate antagonist and pyrimidine analogues); antimicrotubular agents which prevent cell growth by blocking mitosis by disrupting chromosome movement during mitosis (topoisomerase II inhibitors, topoisomerase I inhibitors, taxanes and vinca alkaloids); cytotoxic antibiotics with diverse mechanisms of reaction (actinomycin D, bleomycin, daunomycin) and various antineoplastic drugs that re-aligning DNA strands and sustaining single-strand breaks (hydroxyurea, asparaginase, mitoxantrone [71]. During cancer treatment, the most important step is to prescribe the proper dose of chemotherapeutics

for each individual cancer patient. Optimum between the dose that will cause the minimum side effects and the highest effectiveness should be achieved [72].

1.3.2 Pharmacokinetics

The main branches of pharmacology are pharmacokinetics (PK), the study of the absorption, distribution, metabolism and excretion of the administered drug, and pharmacodynamics (PD), the study of how the drug affects the body (desired and undesired effects). PK and PD are essential in the preclinical and clinical trials of a drug's characterization. Since many chemotherapeutics do not react specifically to the tumorous cells (often causing severe side effects), the main goal of pharmacological studies is therapy optimization, the development of targeted drugs and effective dosage regimens [73]. In addition, information about drug distribution throughout the body is an integral part of drug characterization. Such studies tend to measure the body's internal exposure to the drug, so various sites of exposure assessments are used, including serum, plasma, whole blood, saliva and urine [74]. When the drug is intravenously administrated, the most suitable fluid for the drug's characterization is blood, since the drug is rapidly equilibrated within blood cells and serum proteins [75].

In practice, PK evaluation is performed in serum, because it is easier to follow the free drug and its interactions with serum proteins. Finally, the drug distribution provides the data for the elucidation of the mechanism of antineoplastic therapy, the behaviour of the intact drug and the biotransformation processes at physiologically relevant concentrations [76].

To the greatest extent, pharmacological responses and drug efficacy are related to the unbound fraction of the drug. Only an unbound drug fraction can pass through the cell membranes, diffuse between the plasma and the tissues, and interact with the targeted sites [77].

Lately, protein and peptide-based drugs have attracted a lot of scientific attention. The significant advantage of such drugs lies in the protein's tendency to accumulate into malignant tissues to deliver their increased need for amino acids and energy. This approach enables an increased therapy specificity, a higher efficacy and reduced side effects [78].

Therefore, during the drug design, the study of drug distribution and the kinetics of interaction with serum proteins is of crucial importance. For metal-based chemotherapeutics, such information can be acquired by the speciation analysis. First, different species are chromatographically separated, identified, and/or quantified using different detection techniques. The primary demand for reliable speciation analysis is preserving the species integrity during the analytical procedure. In ideal conditions, the sample preparation would not be necessary, which is usually not the case. Most commonly, analysed samples are influenced by high matrix effects (e.g., a high density of human serum), so the samples must be diluted before the analysis [32].

1.3.3 Metal-based complexes in cancer therapy

Among the metal-based complexes for cancer treatment, Pt-based chemotherapeutic, e.g., cisplatin (cis-diaminedichloro-platinum(II)), oxaliplatin ([(1R,2R)-cyclohexane-1,2-diamine](ethanedioato-O,O')platinum(II)) and carboplatin (cis-diammine (1,1-cyclobutanedicarboxylato)platinum(II)), approved by FDA, are still widely used to treat around 50% of patients receiving chemotherapy for cancer [79], [80]. The structures of these main Pt-chemotherapeutics are presented in Figure 3.

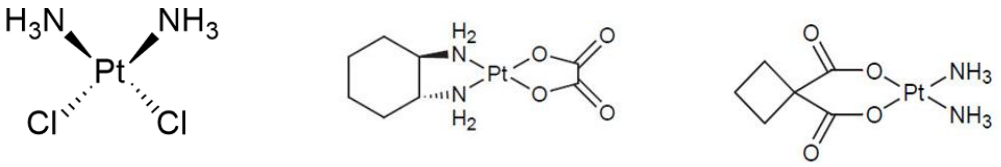

cisplatin **oxaliplatin** **Carboplatin**

Figure 3: Structures of cisplatin, oxaliplatin and carboplatin. Reproduced from freely available images at https://en.wikipedia.org/wiki/.

Pt-based chemotherapeutics are used to treat ovarian, testicular, colon, lung and advanced pancreatic cancers. The primary mechanism of cytotoxicity is similar to alkylating agents, where Pt (a soft Lewis acid) is bound to the DNA (a soft Lewis base), forming inter- and intra-stranded crosslinks. The newly formed crosslinks can cause a change in the double-helix of the DNA structure, thus initiating DNA damage. Such an alteration of the DNA disables the replication and transcription and leads to apoptosis. Although Pt compounds are the core treatment for a wide variety of cancers, this treatment is prone to failure due to the development of inherent or acquired drug resistance and systemic toxicity [81]. To overcome the above-mentioned limitations, new metal-based complexes are being extensively synthesized and studied. Other metal complexes that have entered clinical trials are based on ruthenium (Ru), iron (Fe), copper (Cu), Gold (Au), iridium (Ir) and rhenium (Re) [82], [83].

1.3.4 Ruthenium-based complexes as a possible alternative

This paragraph is based on our published article [84].

With the discovery of cisplatin, scientific interest in synthesising other transition metal-based complexes has increased. Ru-based complexes were one of the most promising alternatives to Pt-based chemotherapeutics. Their main advantage lies in the multifunctional biochemical properties and higher selectivity due to photodynamic, photochemotherapy and photothermal therapy development. The mechanism of action of Ru-based complexes is not similar to Pt-based complexes (triggering DNA inactivation). One of the possible mechanisms of action for the trivalent Ru complexes is its reduction, in cancer cells, by cellular reductants such as ascorbates, into their more active bivalent form. Even though Ru-based drugs have a wide range of intracellular targets, only two Ru-based drugs (Figure 4) are under clinical trials. NKP-1339 (the water-soluble sodium salt of KP1019 [indazolium trans-[tetrachlorobis(1H-indazole) ruthenate (III)]) is in phase 1 under the clinical trial identifier: NCT01415297, developed as a chemotherapeutic and TLD-1433 ([Ru(II) (4,4′-dimethyl-2,2′-bipyridine)2(2-(2′,2″:5″,2‴-terthiophene)-imidazo[4,5-f])]Cl2), which is in phase 2 under the clinical trial identifier: NCT03945162 and shows potential as a photodynamic drug [85].

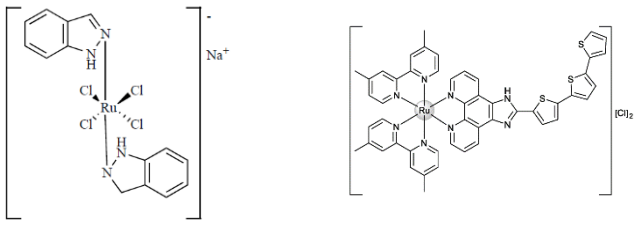

NKP-1339 **TLD-1433**

Figure 4: Structures of NKP-1339 and TLD-1433, adapted from freely images available at http://www.gassergroup.com/anticancer-research/.

Recently, the η6-p-cymene Ru(II) chloride coordination complex with the ligand pyrithione (2-mercaptopyridine N-oxide) **(1)** (Figure 5) was synthetized and investigated for its anticancer activity. The organoruthenium(II) pyrithione complex **(1)** readily reacts with histidine, cysteine and glutathione and shows inhibition properties towards aldo-keto reductase enzymes AKR1C during *in vitro* studies. The enzymes AKR1C1 and AKR1C3 are two of the possible targets for breast cancers, since they are involved in the development and progress of hormone-dependent cancers [86]. Another study reports that complex **(1)** exhibits inhibitory properties towards glutathione-S-transferase (GST), the critical enzyme in developing drug resistance in cancer cells. Moreover, complex **(1)** does not show cytotoxicity to healthy cell lines and undesirable side effects on a neuromuscular system at pharmaceutically relevant concentrations [87]. Additionally, recent studies have focused on synthesising new chlorido and 1,3,5-triaza-7-phosphaadamantane (pta) organoruthenium(II) analogue complexes with methyl-substituted pyrithiones. Complex [(η6-p-cymene)Ru(1-hydroxypyridine-2(1H)-thionato)pta]PF6 **(2)** (Figure 5) is newly synthesized and under extensive investigations. So far, complex **(2)** was evaluated for its cytotoxicity effects on different cell lines, and IC_{50} values were calculated. The highest antiproliferative effects were observed for the A549 (lung) and SKOV3 (ovarian) cell lines [15].

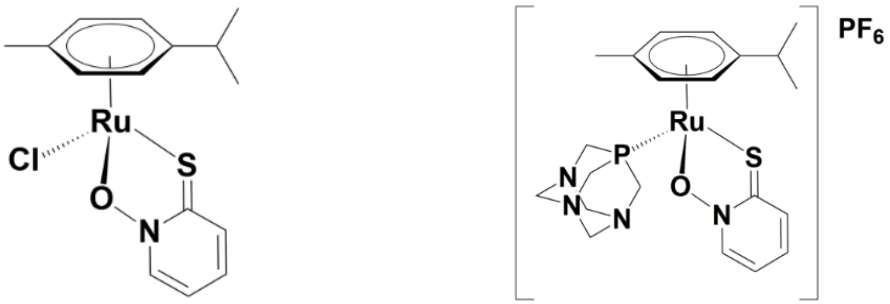

(1) **(2)**

Figure 5: Chemical structures of [(η 6-p-cymene)Ru(1-hydroxypyridine-2(1H)-thionato)Cl] **(1)** and [(η 6-p-cymene)Ru(1-hydroxypyridine-2(1H)-thionato)pta]PF6 **(2)**. Reproduced from reference [82] with permission from MDPI.

Stability studies at biologically relevant concentrations in a cell-culture medium have been performed for complexes **(1)** and **(2)**. Investigations showed that both compounds remained chemically unchanged under biologically relevant conditions [15].

1.4 Copper in Human Serum

This Section 1.4 is based on our published article [88].

Copper (Cu) is the third essential trace metal for all living organisms, after iron (Fe) and zinc (Zn). It is dominantly required as a co-factor for many enzymes such as ceruloplasmin (Cp), superoxide dismutase, cytochrome c oxidase, dopamine β-hydroxylase and many others [89]. Cu can be found in all body tissues and, together with Fe, plays a vital role in the formation of red blood cells and the optimal functioning of the nervous and immune systems [90]. Diet introduces copper to the human body, while faeces and urine excrete it. Total Cu concentration in the human body varies from 50 to 100 mg, primarily found in muscle and liver, while the concentration of Cu in human serum ranges from 500 to 1000 ng mL^{-1} [91]. The highest amount of Cu in human serum, around 90%, is firmly bound to the ceruloplasmin (Cp), while the rest is an exchangeable fraction bound to HSA and amino acids [92].

1.4.1 Ceruloplasmin

Cp is an acute-phase glycoprotein with a single polypeptide chain consisting of 1046 amino acids and 7-8% carbohydrates, exclusively found in the plasma of vertebrates [93]. It is mainly synthesized in the liver and metallated with Cu in the human body. Besides the liver, Cp is synthesized in many tissues, including the brain, lung, spleen and testis [94]. Average Cp concentration in human serum of healthy population varies between 200 to 500 mg/L. Cp has crucial physiological roles. Primarily, it is the main Cu-carrying protein that regulates Cu homeostasis and serves as ferroxidase to export Fe from tissue stores and cells by oxidating Fe^{2+} to Fe^{3+} [95]. So, it is also essential for Fe transport and metabolism and prevents radical oxygen formation [96], [97]. An X-ray structural study showed six non-exchangeable Cu binding sites oriented toward the protein interior and two additional exchangeable Cu binding sites [98].

Figure 6: Structure of Cp obtained by X-ray diffraction (Reproduced from Protein data bank, freely available at https://www.rcsb.org/structure/2J5W).

Holo Cp (Cu ions bound to Cp) has a half-life of 5.5 days. In holo Cp, studies showed that Cu ions are non-exchangeably bound. About 10% of total Cp in the healthy population is present in the apo form (without Cu ions bound to Cp), with a shorter half-life of around five hours [99]. The expression of Cp is known to be altered in some medical conditions. Metabolic disorders of Cp are noted for a few neurodegenerative diseases [100]. Altered Cp concentrations were found in aceruloplasminemia and Wilson's, Menkes, Alzheimer's and

Parkinson's disease [101]–[108]. Additionally, similar observations were found in rheumatoid arthritis, inflammation, T1D diabetes type 1, and chronic hepatitis B [109]–[112]. Cp can serve as a prognostic biomarker for various cancers, such as breast, bladder and bile duct cancer [113]–[115]. Cp is also proposed as a biomarker for ovarian cell carcinoma and lung adenocarcinoma [116]–[118].

1.4.1.1 Disorders related to Cp expression

In the human population, Cu toxicity is related to its impaired transportation due to metabolic disorders. Recessive disorders that are referred to affect Cu transport throughout the body and Cp synthesis are aceruloplasminemia, Menkes (MD) and Wilson disease (WD) [119].

Aceruloplasminemia is a rare neurodegenerative disorder with a prevalence of about 1 in 2,000,000 cases. It is caused by the entire absence of Cp ferroxidase activity, which leads to Fe accumulation in the brain and other internal organs. Fe accumulation triggers various medical conditions, e.g., Diabetes Mellitus and retinal degeneration, neurological signs and symptoms such as dementia, and involuntary movements. Diagnosis of aceruloplasminemia is based on the absence or low serum Cp concentrations, low serum Fe and hepatic Fe overload. Aceruloplasminemia is treatable with Fe chelators [101], [120], [121].

MD is caused by mutations in gene ATP7A, resulting in the reduced activity of brain enzymes that have Cu as a cofactor and consequently cause Cu and Cp serum level deficiency. According to estimations, MD has an incidence rate of 1 in 300 000 new-borns in Europe, with a fatal outcome by age three [104], [122].

On the other hand, Wilson disease (WD) has a prevalence of 1 in 30 000, and it is more frequent in the Asian population. WD is triggered by a genetic mutation in the ATP7B gene. ATP7B mutation disables cuprous (Cu^{+}) and cupric (Cu^{2+}) ions from attaching to the Cp in the liver and their excretion into the bile. Thus, whether Cu is poorly attached to the Cp or accumulated in the liver, causing hepatic failure, or Cu can be stored in the other organs, especially in the brain, cornea and kidneys, causing severe health issues. Usually, symptoms are presented at 10 to 20 years old, but due to their diversity, WD diagnosis is delayed. Among other clinical characteristics, WD diagnosis is based on elevated concentrations of 24 h Cu in the urine, increased total liver Cu level and Cp serum levels lower than 100 mg/L. However, WD is a slow, progressive, but treatable disease if it is diagnosed in time. Effective medical therapies such as chelators and the use of Zn salts are available, providing health-related quality of life and life expectancy close to that of the healthy population [123].

Since Cp-related disorders are highly treatable, the development of prenatal tests and early screening methods are under investigation [105], [106].

1.4.1.2 Analytical methods for ceruloplasmin determination

In routine clinical practice, Cp in human serum or plasma is usually determined by immunologically based methods, i.e., immunoturbidimetry and immunonephelometry. The main disadvantage of these methods lies in their non-specificity, since the holo form cross-reacts with apo Cp, so both forms of Cp are simultaneously measured. The latter is not of medical relevance since it is not an enzymatically active form. Additionally, there is still a high demand for the standardization of Cp measurements in laboratory medicine, but the biggest issue is the lack of a reference material [124], thus making measurement traceability and any laboratory intercomparison practically impossible. Another obstacle is the instability of the Cp standard [125].

To this end, speciation analysis using various separation techniques hyphenated to the ICP-MS showed great potential for clinical practice. A breakthrough was made by Inagaki

et al., who studied the speciation of protein-binding Cu and Zn in human serum by chelating pre-treatment for the removal of loosely bound Cu and Zn species, and the remaining supernatant, which contained Cu-Cp and Zn-α_2-macroglobulin were analysed by SEC-ICP-MS [126]. In addition, Lopez-Avila et al. determined the Cp in human serum by SEC-ICP-MS after the offline purification step with the immunoaffinity column by eliminating six highly abundant proteins (HSA, Tf, IgG, IgA, haptoglobin and antitrypsin) that might overlap Cp on the SEC column. The method was able to separate and quantify Cu-Cp and free Cu in purified human serum samples [127]. Moreover, Kobayashi et al. developed a method for the direct analysis of Cp in human serum by SEC-ICP-MS and proposed it as a diagnostic tool for WD [128]. Finally, Bernevic et al. developed a method for the selective determination of Cp in human serum by online immunocapture using an anti-Cp affinity column coupled to ICP-MS. The obtained data correlated with the offline enzyme-linked immunosorbent assay (ELISA) [129]. One of the biomarkers for WD, the determination of relative exchangeable Cu, present as a percentage of the exchangeable to the total serum Cu, was proposed. This method could be used for the early diagnosis of WD and other Cu-related medical conditions [102]. Quarles Jr. et al. developed a fast and specific method for separating and quantifying the Cu fraction bound to proteins and extractable Cu using automated sample preparation and the Elemental Scientific CF-Cu-02 column, packed with negatively charged resin that can tightly bound Cu, so the Cu bound to proteins was eluted without retention on the column, with the solvent front, while the extractable Cu retained on the column and eluted at around the third minute. ICP-MS was used to detect the separated Cu species, and the sample-to-sample analysis took 6 minutes [130]. Another possibility lies in using a strong anion exchange column coupled to the ICP-MS, and such a setup was used by Solovyev et al. to study WD, where they managed to separate Cu-Cp from the Cu-HSA fraction in one chromatographic run [33].

Finally, for the diagnosis of WD, various liver diseases and inflammation processes, the Cu isotopic composition was determined by multi-collector ICP-MS (MC-ICP-MS) after the chromatographic isolation of Cu using a strong anion exchange resin AG-MP-1 [131]–[133].

1.5 ICP-MS

The separated species can be detected offline and online. Online detection is preferable due to the better selectivity and the shorter time of analysis. Among the various element-specific detectors, ICP-MS (inductively coupled plasma mass spectrometry) is widely used due to the multi-elemental applicability, high sensitivity (low backgrounds, which result in a very low limits of detection (LODs) and limits of quantifications (LOQs). In general, the LODs of most elements are below 0.01 µg L^{-1}. Another great advantage is the wide analytical working range and the possibility of relatively easy hyphenation to different separation systems (e.g., gas and/or liquid chromatography). Using ICP-MS, different isotopes of the same element can also be measured, making it suitable for the isotope dilution (ID) technique for quantifying trace amounts of the separated elemental species [134].

1.5.1.1 Quantification by ID-ICP-MS

So far, the ID-MS quantification technique is one of the most accurate approaches for elemental speciation analysis. The only condition for ID quantification is that the element of interest has at least two stable isotopes. The ID technique is free from physical interferences, so the signal drift and matrix effect are not issues. Consequently, the use of

an internal standard is unnecessary. In determining the total element concentration by ID, a known amount of the same element with an altered isotopic composition (enriched isotopic spike) is added to a sample with an unknown amount of an element. After equilibration, a new ratio between the isotopes of the element of interest is established in the mixture. The concentration of an element in the isotopically diluted sample with ICP-MS can be calculated by measuring the ratio in the sample [135]. There are two different approaches available, i.e., species-specific and species-unspecific ID. In species-specific ID, the species of the added isotopically enriched element is the same as the analyte; for example, the group of Goenaga-Infante for the quantification of carboplatin adducts with HSA prepared enriched ^{194}Pt carboplatin-HSA as a species-specific standard for ID analysis [55]. This is considered the most accurate method of quantification. The species-unspecific method is used whenever performing an analysis of an unknown species or if the isotopically enriched standard is impossible to prepare. This method enables the post-column ID of separated species. After measurement, mass flow versus time is plotted, and the species are quantified by integrating the peaks. The mass flow is calculated according to equation 1. C_{Sp} is the concentration of the spike, d_{Sp} is the density of the spike, f_{Sp} is the sample flow rate, AW_S is the molar mass of the sample, AW_{Sp} is the molar mass of the spike, A_{Sp}^{b} is the isotopic abundance of the enriched isotope in the spike, A_S^a is the isotopic abundance of the targeted isotope in the sample, Rm is the isotope ratio a/b in the mixture, where a is the most abundant isotope in the sample and b is the most abundant isotope in the spike, R_S is the isotope ratio b/a in the sample, and R_{Sp} is the isotope ratio a/b in the spike [136].

$$MF_S = C_{Sp}\ f_{Sp}\ \ d_{Sp}\frac{AW_S}{AW_{Sp}}\frac{A_{Sp}^{b}}{A_S^{a}}\left(\frac{R_m\text{-}R_{Sp}}{1\text{-}R_mR_S}\right) \qquad (1)$$

Chapter 2

Aims and Hypothesis

As an integral part of the preclinical and clinical trials of candidate drugs for cancer treatment, pharmacokinetics plays an important role. To evaluate the effectiveness of a Ru-based candidate drug it is necessary to investigate the distribution of the Ru species in spiked human serum and study the kinetics of interaction for Ru-based chemotherapeutics with serum proteins. For this purpose, the concentrations of intact Ru drug and its species bound to serum proteins need to be determined. For efficient chromatographic separation, CLC on monolithic discs may be used.
Therefore, the aims of the doctoral thesis related to the investigation of the Ru species' interactions in with human serum proteins were:

- To optimize the analytical method for the speciation of Ru-based candidate drugs in human serum by using CLC monolithic chromatography with ICP-MS detection
- To apply the optimized speciation analysis method to the investigation of the kinetics of Ru-based candidate drugs with main serum proteins (Tf, HSA and IgG)

Cu-Cp can be used as a potential biomarker in cancer diagnosis. For this purpose, it is necessary to develop reliable, new analytical method for its determination.
Therefore, the aims of the doctoral Thesis related to the investigation of the Cu-Cp concentrations in human serum were:

- To develop a new analytical method based on the 2D chromatographic separation of Cu species using a CLC monolithic column, which consists of a short-bed immunoaffinity CIMmic α-HSA and CIMmic DEAE disks assembled in a single housing, in a single chromatographic run
- To identify the separated serum proteins by UV detection and to quantify the separated Cu species by post-column isotope dilution (ID)-ICP-MS
- To apply the developed method for the speciation of Cu in the human serum of healthy individuals, transplanted renal patients and cancer patients

Chapter 3

Materials and Methods

3.1 Ruthenium Speciation

The text related to Section 3.1 is based on our published article [84].

3.1.1 Reagents and materials

Ultrapure water (18.2 MΩ cm) was obtained from a Direct-Q 5 Ultrapure water system (Millipore Watertown, MA, USA). All chemicals were of analytical reagent grade. Human serum apo-transferrin (Tf), human serum albumin (HSA) and γ-globulins (IgG) were purchased from Sigma-Aldrich (Steinheim, Germany).

Merck (Darmstadt, Germany) stock Ru solution (1000 ± 8 mg L^{-1} in 7% HCl) was used for the preparation of calibration standard solutions for the determination of the total Ru concentrations in serum samples spiked with Ru-based chemotherapeutics. To control the stability of the ICP-MS, Rh (1000 ± 2 mg L^{-1} in 5 % HNO_3), purchased from Merck, was aspirated along with the sample into the plasma using a peristaltic pump via a T-piece.

For the preparation of buffers and eluents in the chromatographic separation 2-amino-2-(hydroxymethyl)propane-1,3-diol (Tris) buffer, sodium hydrogen carbonate ($NaHCO_3$), ammonium chloride (NH_4Cl) and acetic acid (AcOH), purchased from Merck, were used.

Chromatographic supports of CIM Protein G disk were cleaned with AcOH, while of CIM DEAE disk with Merck sodium hydroxide (NaOH) and Merck sodium chloride (NaCl) [35].

Complex [(η^6-*p*-cymene)Ru(1-hydroxypyridine-2(1H)-thionato)Cl **(1)** (M=396.9 g mol^{-1}) and complex [(η^6-*p*-cymene)Ru(1-hydroxypyridine-2(1H)-thionato)pta]PF_6 **(2)** M=663.6 g mol^{-1} were prepared according to the procedure described by Kladnik et al [15].

A Ru-enriched isotope (^{99}Ru metallic plate, 15 mg) was obtained from Oak Ridge National Laboratory (Oak Ridge, TN, USA).

3.1.2 Instrumentation

Chromatographic separations were performed on an Agilent (Tokyo, Japan) series 1260 infinity quaternary HPLC pump equipped with a Rheodyne model 7725i (Cotati, CA, USA) injector fitted with a 100 µL injection loop and a software-controlled six-port valve. An UV-Vis Agilent 1260 infinity series variable wavelength (VWD) detector was used for the absorption measurements at 278 nm.

For the separation of the Ru species, one CIM Protein G and one CIM DEAE monolithic disk, both from BIA Separations d.o.o. (Ajdovščina, Slovenia), were assembled into one housing, forming a CLC monolithic column. A CIM disk (dimensions 12 mm and

length 3 mm, bed volume 0.34 mL) consisted of a poly (glycidyl methacrylate-co-ethylene dimethacrylate) highly porous monolithic polymer. The CLC column was connected to the HPLC system so that the mobile phase first rinsed the CIM Protein G disk and afterwards the CIM DEAE disk.

The outlet of the column was coupled online with an UV-Vis and an Agilent 7900 ICP-MS instrument. ICP-MS was also used for the determination of the total Ru concentrations in the serum samples. The data was processed with Agilent MassHunter software. The ICP-MS operating parameters were optimized for plasma robustness and to introduce the minimum amounts of salts used in the separation procedure. The tuning of the instrument was performed daily, prior to the analysis.

Table 1: ICP-MS operating parameters.

Parameter	Type/Value Ru speciation analysis	Type/Value Analysis of total Ru content
Sample introduction		
Nebuliser	Miramist	Miramist
Spray chamber	Scott	Scott
Skimmer and sampler	Ni	Ni
Plasma conditions		
Forward power	1550 W	1550 W
Plasma gas flow (Ar)	15.0 L min^{-1}	15.0 L min^{-1}
Carrier gas flow (Ar)	0.45 L min^{-1}	1.05 L min^{-1}
Dilution gas flow (Ar)	0.75 L min^{-1}	/
Make up gas flow (Ar)	/	0.10 L min^{-1}
Total carrier gas flow	1.20 L min^{-1}	1.15 L min^{-1}
He gas flow	4.3 mL min^{-1}	4.5 mL min^{-1}
Omega bias	-110 V	-120 V
Cell entrance	-40 V	-40 V
Cell exit	-60 V	-60 V
Deflect	3.8 V	3.0 V
Plate bias	-60 V	-60 V
Sample uptake rate	1.0 mL min^{-1}	0.3 mL min^{-1}
Data acquisition parameters		
m/z of isotopes monitored	^{99}Ru, ^{101}Ru	^{101}Ru
m/z of internal standards*	^{103}Rh	^{103}Rh
Total acquisition time	1080 s	/

*In speciation analysis, internal standards were not used when the ID-ICP-MS procedure was applied.

A Mettler Toledo MS104 (Zürich, Switzerland) analytical balance was used for the weighing. A WTW (Weilheim, Germany) 330 pH meter was employed to determine the pH.

3.1.3 Methods

3.1.3.1 Sample preparation

To check the separation of serum proteins on the CLC column, a mixture of standard serum proteins (25 g L^{-1} of HSA, 5 g L^{-1} of IgG and 2.5 g L^{-1} of Tf) was dissolved in buffer A, and diluted five times with buffer A before the analysis.

Before the speciation analysis, approximately 5 mg of complex **(1)** was dissolved in 1 mL of MeOH, and appropriately diluted with buffer A, so that the final concentration of MeOH was 0.3%. For the preparation of the complex **(2)** solution, about 5 mg of complex **(2)** was dissolved in 1 mL of water, appropriately diluted with buffer A.

Human serum was obtained from a transplanted renal patient by venous puncture after informed consent was obtained. Approximately 300 mL of whole blood was collected into a Pyrex glass container without additives. Blood aliquots were transferred into 20 mL polyethylene tubes and centrifuged for 10 min at 855 *g*. Serum aliquots were transferred to 2 mL polyethylene tubes and stored at -20 °C. Before analysis, the samples were equilibrated at room temperature.

For the kinetic studies, serum was spiked with complex **(1)** or complex **(2)**, so that the final concentration of Ru in the spiked samples ranged from 0.396 to 4.14 µg mL^{-1}. Samples were incubated at 37 °C from 5 min to 48 h, and diluted five times with buffer A before the speciation analysis.

3.1.3.2 Buffer preparation

Buffer A consisted of 50 mmol L^{-1} Tris-HCl, 30 mmol L^{-1} $NaHCO_3$ and 10 mmol L^{-1} NH_4Cl, pH 7.4. Buffer B was composed of buffer A + 2 mol L^{-1} M NH_4Cl, pH 7.4. Eluent C was 0.5 mol L^{-1} AcOH, pH 2. Buffer D was 0.2 mol L^{-1} Tris-HCl, pH 7.4.

0.1 mol L^{-1} HCl was used for the pH adjustment of buffer A, while for the buffer B, 1-M NaOH was used.

3.1.3.3 Preparation of ^{99}Ru-enriched isotope

The declared composition of the enriched ^{99}Ru plate was 0.12 ± 0.02%, 0.12 ± 0.02%, 97.69 ± 0.1%, 0.74 ± 0.03%, 0.48 ± 0.02%, 0.58 ± 0.01% and 0.27 ± 0.02% for isotopes 96, 98, 99, 100, 101, 102 and 104, respectively. For the preparation of the enriched ^{99}Ru stock solution, 15 mg of ^{99}Ru metallic plate was dissolved in 1 mL of *aqua regia* and diluted to 10 mL with an appropriate amount of HCl, so that the final concentration of the HCl was 7%. The concentration in the ^{99}Ru stock isotopic spike solution was determined by the reverse ID-ICP-MS procedure [136]. The concentration was found to be 597 ± 10 µg g^{-1} ^{99}Ru.

3.1.3.4 Chromatographic procedure

Chromatographic separation was carried out at a flow rate of 1 mL min^{-1}. In the first 5 min, isocratic elution with 100% buffer A was applied to elute the unbound Ru-based chemotherapeutic. In the next 9 min, linear gradient elution from 100% buffer A to 50% buffer B followed to separate the Tf from the HSA. Then, isocratic elution with 100% eluent C was applied for 4 min to elute the IgG. The elution of proteins was followed on-line by the UV detection at 278 nm and the separated Ru species detection by ICP-MS. To obtain reproducible chromatographic separation it was crucial to effectively regenerate and equilibrate the CLC column. After separation, the column was regenerated with buffer D for 3 min and in the next 3 min with buffer B at a flow rate of 6 mL min^{-1}. Finally, the

column was equilibrated with buffer A for 5 min at a flow rate 6 mL min^{-1}, followed by elution with buffer A for 0.5 min at a flow rate of 1 mL min^{-1}. The eluents from the regeneration and equilibration steps (flow rate 6 mL min^{-1}) were directed to waste through a software-controlled six-port valve.

Table 2: Chromatographic separation programme.

Time (min)	Eluent				Species separated
	A (%)	B (%)	C (%)	D (%)	
0-5	100				unbound
5-15*	50	50			Tf, HSA
15-19			100		IgG
19-22				100	regeneration
22-25				100	
25-30.5	100				equilibration

*Gradient elution

3.1.3.5 Quantification of total Ru concentration in the spiked human serum

Total Ru concentration in spiked human serum was determined in 10-times diluted samples by ICP-MS using external calibration method.

3.1.3.6 Quantification of separated Ru species using the post-column ID-ICP-MS

The separated Ru species were quantified using the post-column ID-ICP-MS technique. Isotopically enriched ^{99}Ru was aspirated continuously by a peristaltic pump via a T-piece after the chromatographic separation of the Ru species. For the calculation of the concentration of the eluted Ru-species, the mass flow of Ru was plotted versus time during the chromatographic run. Calculations were made by using equations derived for species-unspecific post-column ID-ICP-MS analysis [136].

If not stated otherwise, all the experiments were performed in duplicate.

3.1.3.7 Cleaning procedure

The cleaning procedure was adopted from a previous study of our group [31]. After approximately 30 serum separations, the CLC monolithic column was dismantled, and cleaning was performed separately for the CIM Protein G and the CIM DEAE disks at a flow rate of 6 mL min^{-1}. The Protein G disk was cleaned with 20 mL, 40 mL and 20 mL of eluent C, buffer D and buffer A, respectively. The DEAE disk was cleaned with 20 mL of 1 mol L^{-1} NaOH, followed by rinsing with 20 mL of water, 20 mL of buffer D, 20 mL of 2 mol L^{-1} NaCl, 20 mL of buffer D and finally with 20 mL of buffer A. After cleaning, the disks were restacked again into the same CIM housing and the CLC column was ready for further use.

3.1.3.8 Data evaluation

Data were extracted using the Agilent 4.5 MassHunter software and further processed with OriginPro 2015 (Northampton, MA, USA) and Microsoft Excel 2019 MSO (Redmond, WA, USA).

3.2 Copper Speciation

The text related to Section 3.2 is based on our published article [88].

3.2.1 Reagents and materials

All the chemicals were of analytical reagent grade. Ultrapure water (18.2 MΩ cm) was obtained from a Direct-Q 5 Ultrapure water system (Millipore Watertown, MA, USA). Human ceruloplasmin (Cp) and human serum albumin (HSA) were purchased from Sigma-Aldrich (Steinheim, Germany).

All reagents used for the separation and cleaning of the chromatographic supports were from Merck (Darmstadt, Germany).

Nitric acid (HNO_3) s.p. purchased from Carlo Erba (Milan, Italy) and hydrogen peroxide (H_2O_2) s.p. (Sigma-Aldrich) were used to digest the samples. Citric acid p.a., was purchased from Merck.

Merck stock Cu solution (1000 mg Cu L^{-1} in 3% HNO_3) was used to prepare the calibration standard solutions.

Copper oxide powder enriched with mass 65 (^{65}CuO) was obtained from Nakima Ltd (Yehud-Monosson, Israel). The declared composition of the enriched ^{65}CuO powder is 0.33 ± 0.03% and 99.67 ± 0.03% for the 63 and 65 isotopes, respectively.

Seronorm™ trace element serum L^{-1} quality control material was purchased from SERO AS, (Billingstad, Norway).

3.2.1.1 Instrumentation

An Agilent (Tokyo, Japan) series 1200 HPLC system with a quaternary pump was used for the chromatographic separations. It was equipped with an Agilent 1260 Bio-inert Manual Injector valve, fitted with a high-density polyethylene (HDPE) 20 µL injection loop.

For the separation of the Cu species in the serum, two 0.1 mL Convective Interaction Media (CIM) CIMmic™ immunoaffinity α-HSA disks and one 0.1 mL CIMmic weak anion-exchange DEAE disk from BIA Separations d.o.o. (Ajdovščina, Slovenia) were assembled in a single housing, forming a Conjoint Liquid Chromatography (CLC) monolithic column.

A UV-Vis Agilent 1200 series with a multiple-wavelength (MDW) detector was used to follow the protein elution at 278 nm. The outlet of the detector was coupled online to a single quadrupole ICP-MS, model 7700x from Agilent Technologies (Tokyo, Japan). ICP-MS was also used to determine the total Cu content in human serum samples. The ICP-MS operating parameters were optimized for plasma robustness and for introducing the minimum amounts of salts used in the chromatographic separation procedure. To eliminate polyatomic interferences arising from sample matrix and plasma constituents at m/z 63 and m/z 65 the High Energy Collision Mode (HECM) was applied, using helium as a collision gas [137]. The ICP-MS operating parameters are provided in Table 3.

Table 3: ICP-MS operating parameters.

Parameter	Type/Value Speciation analysis	Type/Value Analysis of total Cu content
Sample introduction		
Nebuliser	Miramist	Miramist
Spray chamber	Scott	Scott
Skimmer and sampler	Ni	Ni
Plasma conditions		
Forward power	1550 W	1550 W
Plasma gas flow (Ar)	15.0 L min^{-1}	15.0 L min^{-1}
Carrier gas flow (Ar)	0.80 L min^{-1}	1.00 L min^{-1}
Dilution gas flow (Ar)	0.30 L min^{-1}	/
Make up gas flow (Ar)	/	0.20 L min^{-1}
He flow	9.5	4.5
Data acquisition parameters		
m/z of isotopes monitored	^{63}Cu, ^{65}Cu	^{63}Cu
m/z of internal standards*	^{103}Rh*	^{103}Rh
Total acquisition time	960 s	/

*In speciation analysis, internal standards were not used when the ID-ICP-MS procedure was applied.

A CEM Corporation (Matthews, NC, USA) CEM MARS 6 Microwave Acceleration Reaction System was used to digest the serum samples.

A Mettler Toledo MS104 (Zürich, Switzerland) analytical balance was used for the weighing.

A WTW (Weilheim, Germany) 330 pH meter was employed to determine the pH.

3.2.2 Methods

3.2.2.1 Sample preparation

Standard serum proteins were reconstructed in buffer A and were used for the method development. Prior to the chromatographic separations, they were appropriately diluted so as not to exceed the binding capacity of the monolithic disks.

Blood samples were obtained with a venous puncture from six healthy individuals (ages 24 to 65), four transplanted renal patients (ages 30 to 42) and six lung cancer patients (ages 39 to 76). 5 mL of blood from the healthy individuals was taken after informed consent. In the transplanted renal patients, about 300 mL of blood was taken during venous puncture. In clinical practice, this blood is discarded. In the present study, it was used for research purposes after informed consent was obtained.

Blood samples from the lung cancer patients, treated with Pt-based chemotherapeutics, were obtained about 3 weeks after receiving the chemotherapy, with the approval of the ethical committee (Republic of Slovenia, Ministry for Health, document No. 0120-696/2017/4, 22.01.2018) and conducted according to the rules of Good Clinical Practice (Declaration of Helsinki), and informed consent from the patients.

The blood from the healthy individuals and the cancer patients was collected in Becton-Dickinson vacutainers without additives, while the blood of the transplanted renal patients

was gathered in a glass flask. The clot was removed by centrifugation (10 min, 855 g) and the serum in the supernatant carefully collected using a polyethylene pipette, transferred to 2 mL polyethylene tubes and stored in a freezer at -20 °C.

Before the analysis all the samples were thawed and equilibrated at room temperature (T). Prior to the speciation analysis, the serum samples were diluted 15 times with buffer A.

3.2.2.2 Buffer preparation

Buffer A was composed of 50 mmol L^{-1} MOPS, pH 7.4. Buffer B contained buffer A + 2 mol L^{-1} of ammonium chloride (NH4Cl), pH 7.4, eluent C was 0.5 mol L^{-1} acetic acid, pH 2.45 and buffer D consisted of 2 mol L^{-1} MOPS, 2 g L^{-1} EDTA and 1% Tween 20, pH 7.4.

1 M NaOH was used for pH adjustment of buffers A, B and D.

3.2.2.3 Preparation of ^{65}Cu-enriched isotope

12 mg of ^{65}CuO was weighed in a Teflon vessel. 0.5 mL of HNO_3 and 1.5 mL of MilliQ water were added and the samples were subjected to closed-vessel microwave digestion at a maximum power of 1200 W, ramped to T 90 °C for 15 min, held at 90 °C for 5 min, ramped to T 140°C for 10 min, held at 140°C for 15 min, and cooled in the next 30 min. The obtained clear solution was quantitatively transferred into polyethylene graduated tubes and filled to 30 mL with MilliQ water. The Cu concentration in the enriched isotopic standard was determined by reverse ID-ICP-MS.

3.2.2.4 Chromatographic procedure

20 µL of 15 times diluted serum sample or standard serum proteins were injected into the column. The high dilution of the serum samples was necessary to ensure quantitative sample loading and not to exceed the capacity of the α-HSA disks. To retain the Cu-HSA on the α-HSA disks, isocratic elution with 100% buffer A was applied in the first 3 min at a flow rate of 0.3 mL min^{-1}, while the Cu-Cp and Cu-LMM species passed through the α-HSA disks and were retained on the DEAE disk. A linear gradient elution from 100% buffer A to 50% buffer B then followed for 9 min at a flow rate of 0.6 mL min^{-1} to separate the Cu-Cp from the other serum proteins and the LMM-Cu species retained on the DEAE disk. From 12 to 13.5 min a gradual switching of the eluents from 50% A and 50% B to 100% C was applied at the same flow rate, to ensure optimal mixing of the mobile phase for the quantitative elution of the Cu-HSA. Then, the Cu-HSA was eluted from the column by isocratic elution with 100% eluent C for 4 min at a flow rate of 1 mL min^{-1}. During the separation step (16 min), the eluate from the CLC column was passed through the UV detector (278 nm) for protein monitoring and was further introduced to the ICP-MS. Quantification of the separated Cu species was based on the peak area using the post-column ID-ICP-MS technique.

Regeneration and equilibration followed at a flow rate of 1.5 min, according to the procedure given in Table 4. The eluate from the regeneration and equilibration steps was directed to waste through a software-controlled six-port valve.

Table 4: Chromatographic program for the separation of Cu species on the CLC monolithic column.

Time (min)	Eluent				Flow rate (mL min^{-1})	Steps in the chromatographic procedure
	A (%)	B (%)	C (%)	D (%)		
0-3	100				0.3	separation
3-12*	50	50			0.6	
12-13.5	50	50			0.6	
			100		0.6	
13.5-16			100		1.0	
16-20				100	1.5	regeneration
20-25		100			1.5	
25-26				100	1.5	
26-30	100				1.5	equilibration
30-30.5	100				0.3	

*Gradient elution

3.2.2.5 Quantification of total Cu concentration in spiked human serum

For the determination of the total Cu concentration, 0.25 mL of serum was transferred into Teflon vessels. 0.75 mL of MilliQ water, 0.5 mL of H_2O_2 and 0.5 mL of HNO_3 were added and the sample was subjected to closed-vessel microwave digestion at a maxim power of 1200 W, ramped to 120 °C for 15 min, held at 120 °C for 60 min and cooled in the next 20 min. The clear solution was quantitatively transferred into a polyethylene graduated tube and filled to 30 mL with MilliQ water. The same procedure (acids without samples) was used to prepare a blank sample. The Cu concentrations in the digested serum were determined by ICP-MS using matrix-matched standards for the calibration.

3.2.2.6 Quantification of separated Cu species by the post-column ID-ICP-MS

The separated Cu species on the CLC column were quantified using the post-column ID-ICP-MS, monitoring Cu isotopes at *m/z* 63 and 65. The isotopically enriched ^{65}Cu (5.139 ng mL^{-1}) was delivered with a peristaltic pump *via* a T-piece after the separation of Cu species. The mass flow of Cu was plotted versus time during the chromatographic separation and the concentrations of Cu species calculated by means of equations for the post-column species-unspecific ID-ICP-MS analysis.

If not stated otherwise, all the samples were analysed in duplicate.

3.2.2.7 Cleaning procedure

After approximately 25 injections of serum samples, the α-HSA disks were replaced, while the DEAE disk was subjected to rigorous cleaning. The CLC column was dismantled and cleaning was performed for the DEAE disk at a flow rate of 5 mL min^{-1}. First, it was rinsed with 5 mL of water, followed by rinsing with 5 mL of 1 mol L^{-1} NaOH, 5 mL of 2 mol L^{-1}

NaCl and finally with 5 mL of buffer A. After cleaning, the α-HSA and DEAE disks were re-assembled into the same CIM housing and the CLC column was ready for further use.

3.2.2.8 Data evaluation

Data were extracted using the Agilent 5.1 MassHunter software and further processed with OriginPro 2015 (Northampton, MA, USA) and Microsoft Excel 2019 MSO (Redmond, WA, USA).

A simple statistical analysis was carried out to check significant differences in the Cu-Cp, Cu-HSA and total Cu concentrations between the populations of cancer patients and healthy individuals, and the transplanted renal patients and healthy individuals. For this purpose, Student's *t*-test at a 0.05 level of significance was applied.

Chapter 4

Results and Discussion

The results from chapter 4 were published by Marković et al. in peer-reviewed scientific journals [84], [88].

4.1 Ruthenium Speciation

As an integral part of the preclinical and clinical trials of candidate drugs, pharmacokinetics plays an important role. To evaluate the effectiveness of the Ru-based candidate drug it is necessary to investigate the distribution of the Ru species in spiked human serum and study the kinetics of the interaction of Ru-based chemotherapeutics with serum proteins. For this purpose, the concentrations of the intact Ru drug and its species bound to serum proteins need to be determined. For efficient chromatographic separation, CLC on monolithic discs may be used. In the present dissertation, a CLC monolithic column, combing two separation modes, immunoaffinity Protein G and anion-exchange DEAE disks was used to separate the intact Ru-based drug and drug bound to transferrin (Tf), HSA and immunoglobulin G (IgG). The separated Ru species were quantified by post-column ID-ICP-MS. The kinetics of the interaction of the Ru-based chemotherapeutics with serum proteins was also studied.

4.1.1 Optimization of the analytical procedure for the speciation of Ru complexes (1) and (2) on the CLC column

A procedure that was previously developed in our group for the speciation of Pt-based chemotherapeutics on the CLC column [34] was optimized for the investigation of speciation of the Ru-drug candidates. The analytical procedure is described in detail in *3.1.3.4.* Typical chromatograms of the separation of ionic Ru (Ru^{3+}), Ru complexes **(1)** and **(2)** monitored by ICP-MS at m/z 101, and of the mixture of serum proteins followed by UV at 278 nm detection on the CLC column are presented in Figure 7.

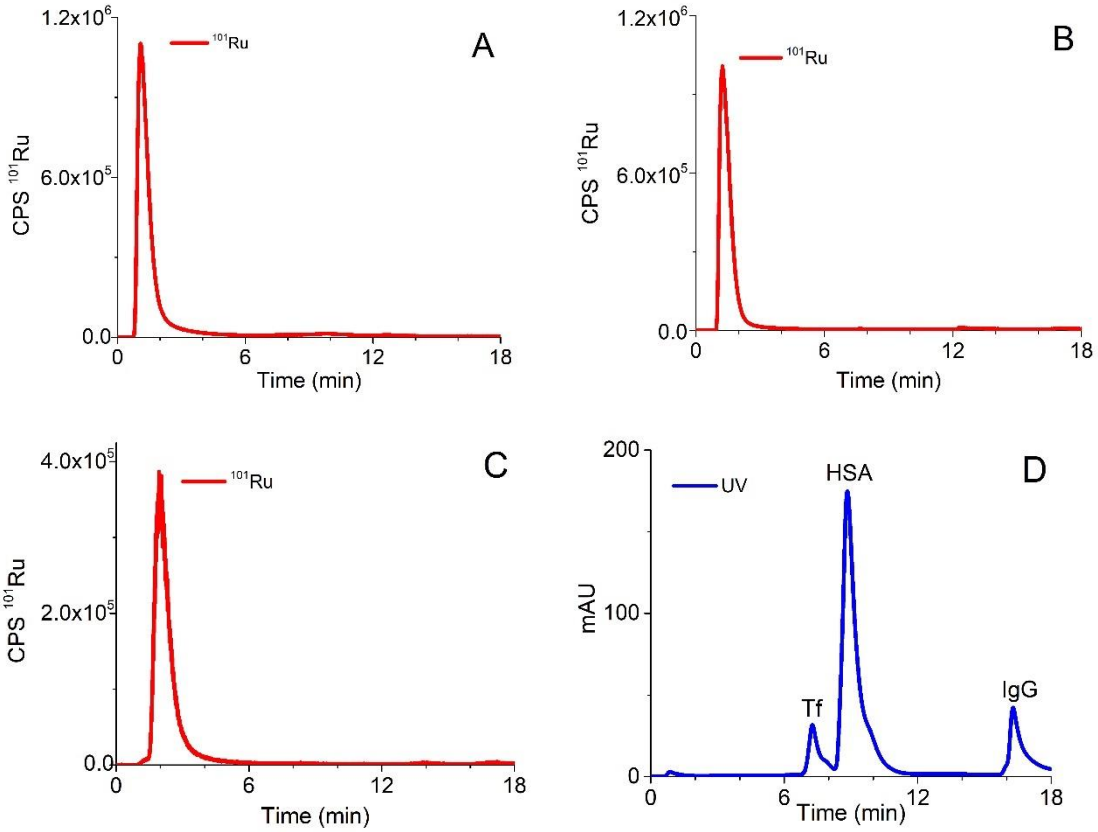

Figure 7: Typical chromatograms for the separation of (A) Ru^{3+} (2 µg mL^{-1} Ru), (B) complex **(1)** (1.64 µg mL^{-1} Ru), (C) complex **(2)** (1.60 µg mL^{-1} Ru) followed by ICP-MS detection at *m/z* 101, and (D) 5-times diluted mixture of standard serum proteins (25 g L^{-1} HSA, 5 g L^{-1} IgG and 2.5 g L^{-1} Tf) monitored by UV at 278 nm.

To prevent the partial adsorption of complex **(2)** on the stationary phase of the CLC column and to enable the separation of unbound Ru species from those bound to serum proteins, 10 mmol L^{-1} NH_4Cl was added to buffer A and isocratic elution with buffer A was applied for 5 min. As can be seen from Figure 7, Ru^{3+} and positively charged complexes **(1)** and **(2)** pass through the Protein G and CIM DEAE disks and are eluted prior to the elution of the main serum proteins. During the gradient elution, from 100% buffer A to 50% buffer B, the Protein G disk retained IgG, while the Tf and HSA were separated on the DEAE disk. Finally, IgG was rinsed from the column by isocratic elution with 0.5 mol L^{-1} AcOH. Data from Figure 7 revealed that the optimized speciation procedure enables the effective separation of positively charged Ru species from the serum proteins.

In the following experiments, a human serum sample was spiked with solutions of complexes **(1)** or **(2)** and the speciation analysis on the CLC column was performed 24 h after incubation at 37 °C. Separation of proteins was followed by UV at 278 nm and monitored by ICP-MS at *m/z* 101 for the Ru species (Figure 8).

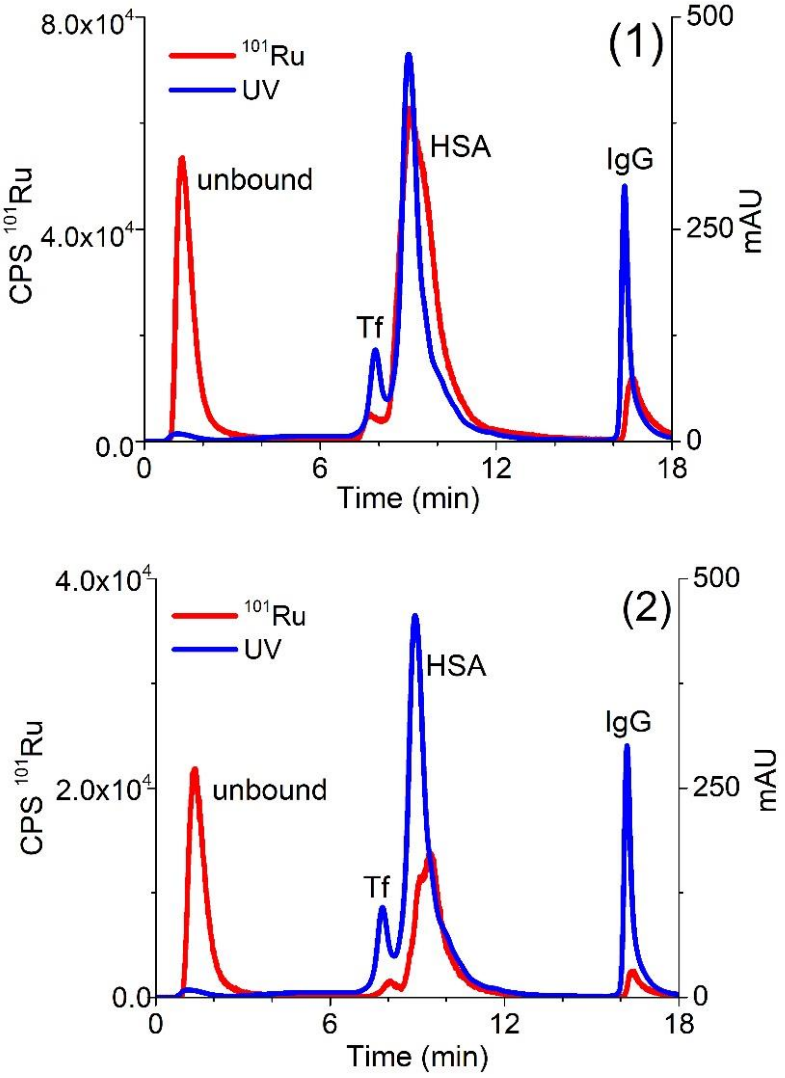

Figure 8: Two-dimensional separation of 5-times diluted human serum spiked with complexes (**1**) (0.760 µg mL^{-1} Ru) or (**2**) (0.396 µg mL^{-1} Ru) on CLC monolithic column 24 h after incubation, followed by UV at 278 nm and ICP-MS at m/z 101 detection.

As evident from the data of Figure 8, the optimized speciation procedure enables the separation of positively charged Ru species (unbound Ru (**1**) and (**2**) complexes) and their adducts with the main serum proteins. Presented Ru **(1)** and **(2)** complexes can undergo hydrolysis; therefore, their Ru-OH and Ru-OH_2 species in the unbound fraction might be present in the solution as well. Apart from the mentioned hydrolysis products, there is a possibility of interference from Ru complexes with some LMM components from the serum, too. We are aware of the importance of identifying the mixture of Ru species that might be present in the solution. However, in this study we focused on the kinetics and the extent of binding of Ru species to HSA, Tf and IgG that can be studied by techniques described herein. For the exact identification of the mentioned species, other methods should be applied.

4.1.1.1 Quantification of separated Ru species on the CLC column using post-column ID-ICP-MS

For the quantification of the Ru species separated on the CLC column, the post-column ID-ICP-MS technique was applied. For this purpose, isotopes at *m/z* 99 and 101 were monitored. To calculate the concentrations of the separated Ru species, the mass flow of ^{101}Ru was plotted versus the time during the chromatographic run [136]. The representative chromatograms of the serum sample spiked with complexes **(1)** or **(2)** are presented in Figure 9.

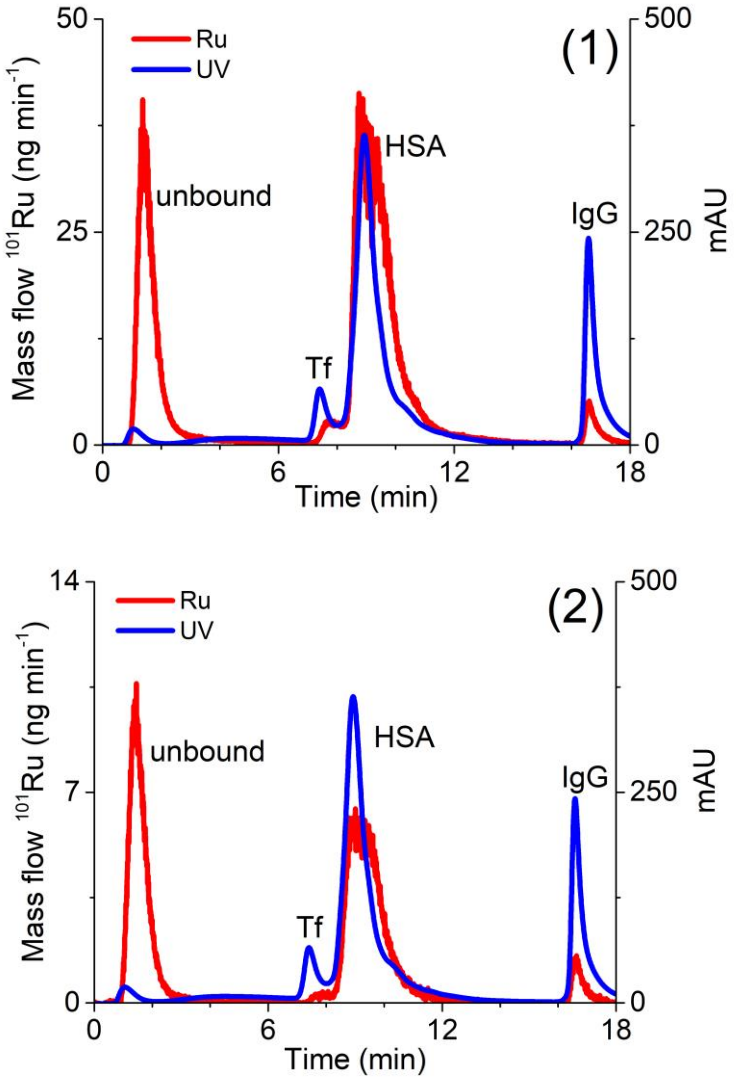

Figure 9: Two-dimensional separation of Ru species in serum sample spiked with complexes **(1)** (4.14 µg mL^{-1} Ru) or **(2)** (0.838 µg mL^{-1} Ru). Speciation analysis consisted of separation on the CLC monolithic column (24 h after incubation in 5-times diluted serum samples) and on-line UV at 278 nm and ICP-MS detection. Ru mass flow is based on measurement of isotope ratios *m/z* 99 and 101.

4.1.1.2 Kinetics of the interaction of Ru complex (1) and (2) with human serum proteins

For a better understanding of the drug–protein interaction, kinetic studies of the association of complexes **(1)** and **(2)** with the serum proteins were carried out. For this purpose, human serum was spiked with complexes **(1)** or **(2)** in a concentration of 0.760 µg mL^{-1} Ru or 0.396 µg mL^{-1} Ru, respectively. Expressed as molar concentrations, the spiking concentration of complex **(1)** was 2.99 mmol L^{-1}, while that of complex **(2)** was 2.60 mmol L^{-1}. Similar molar concentrations of complexes **(1)** and **(2)** enabled the comparison of the data from the kinetic study. The samples were incubated at 37 °C for 5 min, 30 min, 1 h, 2 h, 4 h, 6 h, 24 h, and 48 h and a speciation analysis was applied using the optimized analytical procedure (section *3.1.3.4*). Separated Ru species were quantified using post-column ID-ICP-MS. The results are presented in Figure 10.

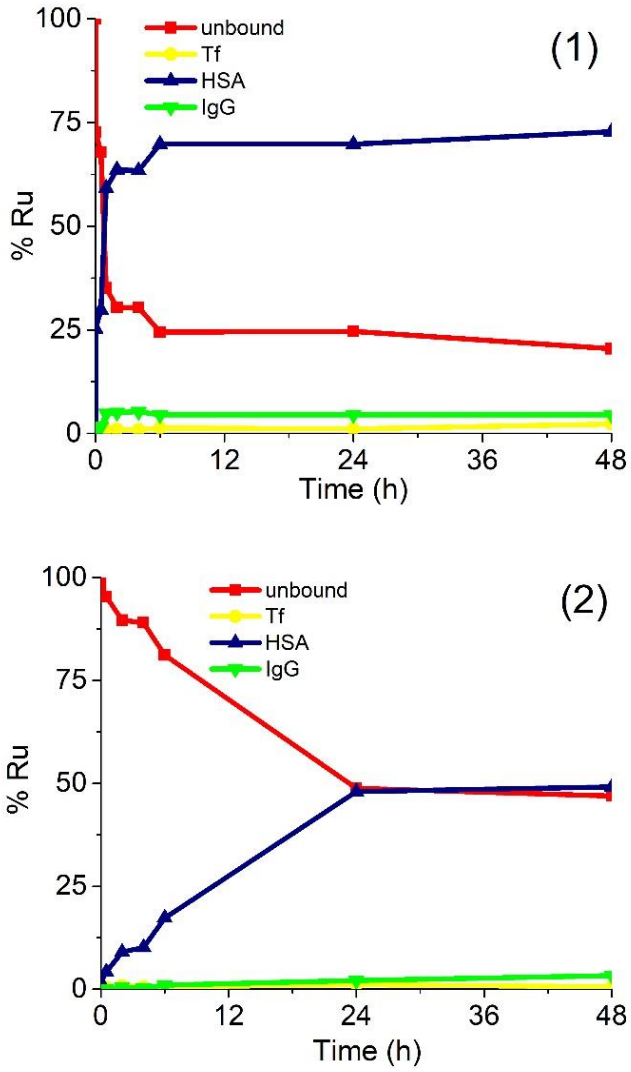

Figure 10: Kinetics of binding of complexes **(1)** and **(2)** to serum proteins. Human serum was spiked with complex **(1)** (0.760 µg mL^{-1} Ru) or **(2)** (0.396 µg mL^{-1} Ru). For separation of the Ru species in 5-times diluted serum samples the CLC monolithic column was used. Their separation was followed by the UV spectrometry at 278 nm and post-column ID-ICP-MS detection.

The data in Figure 10 indicate that both Ru complexes bind mainly to HSA, while their rate of interaction and kinetics are different. Chlorido complex **(1)** rapidly binds to serum proteins. The equilibrium concentrations of the Ru species found in the human serum were reached 6 h after incubation, with around 70% of complex **(1)** bound to HSA and 5% associated with IgG, while 25% of complex **(1)** remained unbound. It can be further seen that the kinetics and the rate of interaction of complex **(2)** with HSA was much slower and less extensive in comparison to complex **(1)**. The equilibrium concentration was obtained 24 h after incubation, with about 50% of complex **(2)** bound to HSA and another 50% as an unbound drug. These data can be compared with the results of a protein-binding study described by Kladnik et al. [15], who investigated the binding of analogous methyl-substituted pyrithione chlorido and pta Ru(II) complexes to BSA. The obtained data reported in this study for chlorido complex **(1)** are in very good agreement with the data obtained for its methyl-substituted pyrithione analogue on BSA, as in both cases the complexes are bound to albumins in around 70%. Further, complex **(2)** binds to HSA with around 50%, whereas its methyl analogue binds to BSA with around 58%. Taking into consideration the small structural changes of both pta Ru complexes and both albumins' data from these two studies are comparable as well [15]. The new findings have again confirmed more in detail that the investigated complexes are partly bound to proteins, but they also exist in their free form. Considering drug design, both forms of complexes must be present in the body for an effective biological response [138]. In many cases, proteins, especially HSA, were proven to act as drug carriers in the body to deliver pharmaceutically active agents to the site of the actions; however, the unbound form must also be present to trigger a pharmacological effect [139]. In this research we have shown that chlorido and pta complexes possess different rates and extent of the binding to the studied proteins and that various substituents importantly influence the kinetic interactions. Similarly, we have previously observed big differences in the biological activity of another chlorido-pta pair of complexes, namely [(η6-p-cymene)Ru(4,4,4-trifluoro-1-(4-chlorophenyl)-1,3-butanedione)Cl] and [(η6-p-cymene)Ru(4,4,4-trifluoro-1-(4-chlorophenyl)-1,3-butanedione)pta]PF6. It seems to be a general trend that the chloride ligand is more easily exchanged with water than the pta ligand, i.e., the chlorido ligand is more labile than pta. This also affects the kinetics of interactions with biomolecules and thus also their biological activity [86], [140], [141].

4.1.2 Analytical figures of merit

4.1.2.1 Column recovery

Column recovery was checked with a Ru speciation analysis in a five-times diluted human serum spiked with complexes **(1)** or **(2)** after incubation at 37 °C for 24 h using post-column ID-ICP-MS for quantification of the separated Ru species. The column recoveries were calculated as the ratio between the sum of the concentrations of the Ru species in the fractions eluted and the Ru concentration in the spiked serum injected into the column. The results are presented in Table 5.

Table 5: Concentrations of Ru species in human serum spiked with complexes (1) or (2). Ru species were separated on the CLC column and their concentration determined by ICP-MS, using post-column ID-ICP-MS. Column recovery was calculated as the ratio between the sum of the concentrations of Ru species in the fractions eluted and the Ru concentration in the spiked serum injected onto the column.

	Ru Injected (µg mL^{-1})	Unbound Ru (µg mL^{-1})	Ru-Tf (µg mL^{-1})	Ru-HSA (µg mL^{-1})	Ru-IgG (µg mL^{-1})	Ru Eluted (µg mL^{-1})	Column Recovery (%)
(1)	4.14±0.08	1.28±0.01	0.038±0.001	2.48±0.02	0.125±0.002	3.92±0.01	95±1
(2)	0.838±0.025	0.386±0.004	0.014±0.001	0.443±0.005	0.027±0.001	0.869±0.008	104±3

The column recoveries were 95% and 104% for the serum spiked with complexes **(1)** or **(2)**, respectively. These data confirm that the optimized CLC procedure enables a quantitative elution of the separated Ru species from the column.

4.1.2.2 Repeatability and reproducibility of the measurements

The repeatability of the measurements was evaluated using six consecutive speciation analyses of human serum spiked with complexes **(1)** or **(2)** after incubation for 24 h. Five-times diluted samples were injected onto the CLC columns. The reproducibility of the measurement was calculated from a set of six consecutive speciation analyses of the same sample analysed on another day. The data are presented in Table 2.

Table 6: Repeatability and reproducibility of measurements for the speciation of Ru in serum samples spiked with complexes **(1)** (4.14 µg mL^{-1} Ru) or **(2)** (0.838 µg mL^{-1} Ru) on CLC column.

	Complex **(1)**		Complex **(2)**	
Ru species	Repeatability RSD (%)	Reproducibility RSD (%)	Repeatability RSD (%)	Reproducibility RSD (%)
Unbound Ru	1.6	6.9	1.2	4.4
Ru-Tf	3.3	5.2	1.6	6.3
Ru-HSA	0.63	1.4	2.9	3.3
Ru-IgG	2.7	4.9	3.8	4.0

As can be seen from the data in Table 6, good repeatability and reproducibility of the measurement were observed for the Ru species separated on the CLC column, with RSDs for particular Ru species ranging from 0.6 to 3.8% and from 1.4 to 6.9%, respectively.

4.1.2.3 Limit of detection, limit of quantification and linearity of measurement

The limit of detection (LOD) and limit of quantification (LOQ) for the determination of the Ru species were calculated as the concentration that provides a signal (peak area) equal to $3s$ and $10s$ of a blank sample in the chromatogram, respectively. For the calculation of the LODs and LOQs, eight blank samples of unspiked human serum were injected onto

the CLC column. The LODs and LOQs for the separated Ru species are presented in Table 7.

Table 7: Limits of detection (LOD) and limits of quantification (LOQ) for separated Ru species on the CLC monolithic column with ICP-MS detection.

Ru Species	LOD (ng mL^{-1} Ru)	LOQ (ng mL^{-1} Ru)
Unbound	0.32	1.1
Ru-Tf	0.12	0.40
Ru-HSA	1.6	5.3
Ru-IgG	1.1	3.6

As can be seen, low LODs (<1.6 ng mL^{-1} Ru) and LOQs (<5.3 ng mL^{-1} Ru) were obtained for the separated Ru species.

The linearity of the measurement, for all the Ru species separated on the CLC column, was confirmed over the concentration range from LOQs to 100 ng mL^{-1} Ru (correlation coefficient (R^2) better than 0.997).

The performances of the optimized speciation procedure allow quantitative kinetic studies of the binding of Ru complexes **(1)** and **(2)** to human serum proteins.

4.2 Copper Speciation

Cu-Cp can be used as a potential biomarker in cancer diagnosis. For this purpose, it is necessary to apply reliable analytical techniques for its determination. In the dissertation, a novel analytical method for the speciation of Cu in human serum, which is based on CLC monolithic chromatography with post-column ID-ICP-MS detection was developed. Separation of Cu species was achieved in a single chromatographic run on the column that was constructed by assembling immunoaffinity CIMmic α-HSA and CIMmic weak anion-exchange DEAE disks into a single housing. Separated Cu species were quantified by post-column ID-ICP-MS.

4.2.1 Method development for Cu speciation in human serum

In Cu speciation, the choice of buffer is of great importance. The widely used Tris buffer strongly interacts with Cu^{2+}, forming at neutral pH, dimeric complexes [142]. However, this fact was often ignored in previous publications. Therefore, among the different possible buffers, MOPS was selected for the Cu speciation, since it is one of the zwitterionic aminosulfonic (Good) buffers that do not interfere with the Cu^{2+} ions [143].

First, a weak anion-exchange DEAE disk was used to separate two Cu-binding proteins in human serum, i.e., Cp (molecular weight 132 kDa) from HSA (molecular weight 66.5 kDa). A study was performed with standard serum proteins, so that their final concentrations after dilution with buffer A were high enough to allow UV and ICP-MS detection. Standard serum proteins used in the present study were isolated from human serum. Thus, the serum proteins Cp and HSA naturally contained Cu. HSA (25 g L^{-1}) was 5-times diluted and 20 µL of sample was injected into the DEAE disk. The injection of 20 µL of 5-times diluted standard serum Cp (1 g L^{-1}) followed. The eluate from the disk first passed through the UV detector and was further transferred to the ICP-MS. To separate the serum proteins, isocratic elution with buffer A was applied for 3 min at a flow rate of 0.3 mL min^{-1}, followed by gradient elution from buffer A to 1 mol L^{-1} NH_4Cl in buffer A in

the next 9 min at a flow rate of 0.6 mL min^{-1}. Overlays of two chromatographic separations are presented in Figure 11.

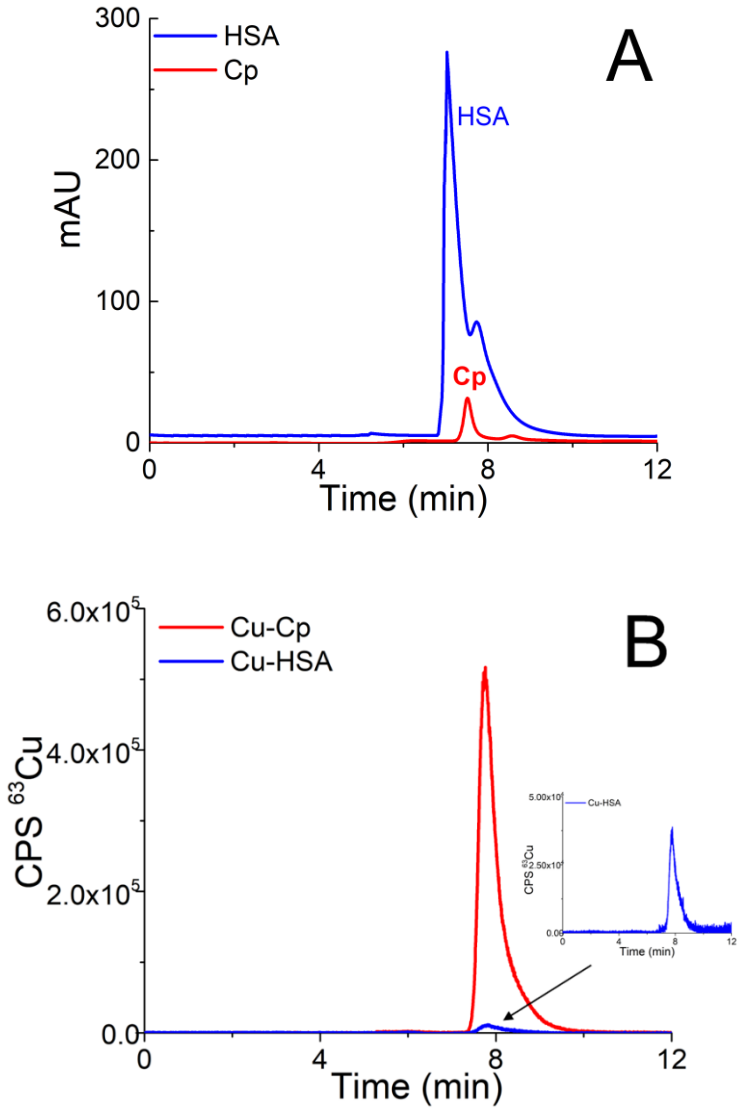

Figure 11: Overlays of chromatograms of 5-times diluted sample of a mixture of standard serum proteins HSA (25 g L^{-1}) and Cp (1 g L^{-1}) on the DEAE disk monitored by (A) UV detection at 278 nm and (B) ICP-MS detection at m/z 63.

As can be seen from Figure 11 A, HSA and Cp are co-eluted. The co-elution of Cu-Cp and Cu-HSA is also evident from Figure 11 B, where ICP-MS detection was applied. As expected, the Cu-Cp peak is much higher than that of the Cu-HSA.

To demonstrate that the greater dilution of the sample does not compromise the integrity of the Cu species, standard serum protein HSA (25 g L^{-1}) was diluted 5- and 15-times and the separation was performed on the DEAE disk. The chromatograms monitored by UV at 278 nm and ICP-MS detection at m/z 63 are provided in Figure 12.

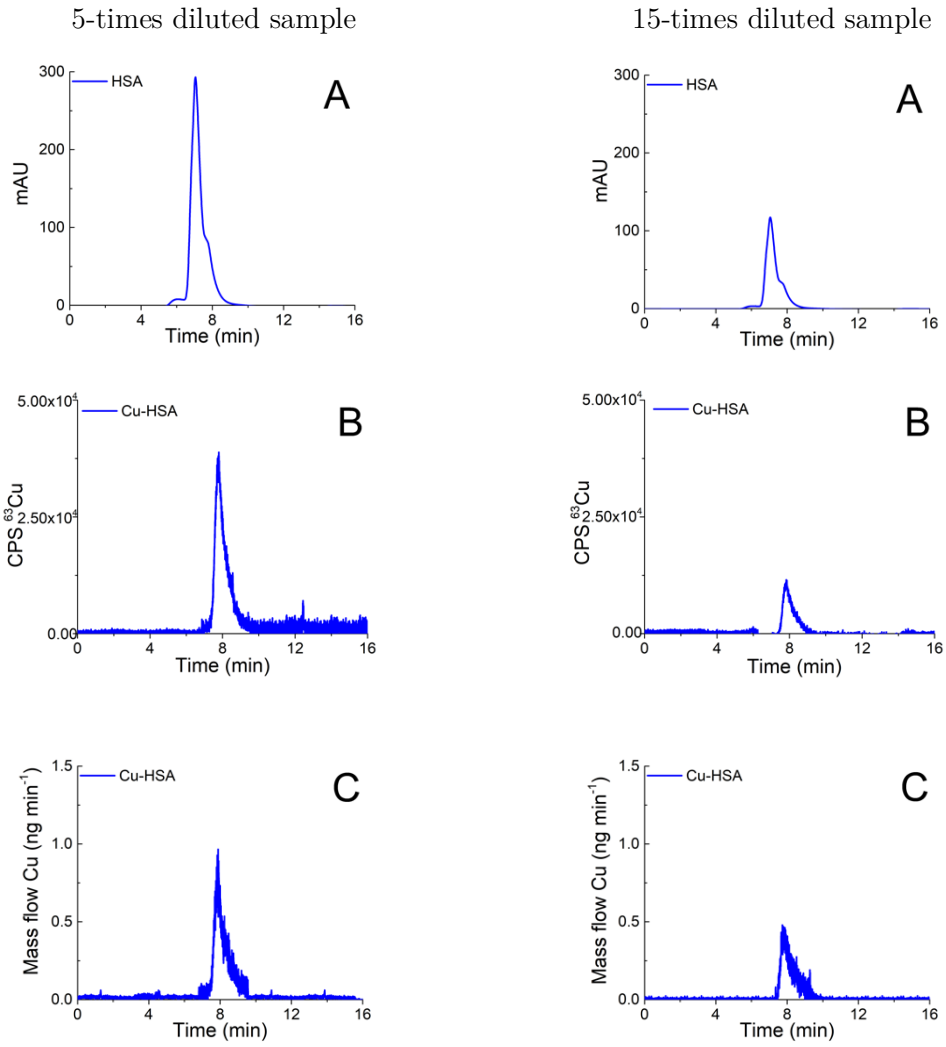

Figure 12: Chromatograms of separation of 5-times and 15-times diluted sample of standard serum protein HSA (25 g L^{-1}) on the DEAE disk monitored by (A) UV detection at 278 nm, (B) ICP-MS detection at m/z 63 and (C) ICP-MS detection. Cu mass flow is based on measurements of isotope ratios m/z 63 and 65.

The data from Figure 12A and 12B indicate that the HSA protein (UV detection) is eluted at the same retention time as the Cu-HSA (ICP-MS detection).

To quantify the separated Cu-HSA species by ICP-MS, the ID technique was applied using equations for the post-column ID-ICP-MS analysis [136]. The mass flow of Cu, based on measurements of the isotopic ratios' m/z 63 and 65, was plotted versus time during the chromatographic run (Figure 12 C).

The concentration of Cu calculated by post-column ID-ICP-MS in the 5-times diluted sample was 146.1 ng mL^{-1}, while in 15-times diluted sample it was 146.3 ng mL^{-1}. Therefore, the 15-times dilution of the sample does not compromise the integrity of the Cu species.

In further steps of the method development, a CLC monolithic column was constructed. The chromatographic conditions were optimized so that the α-HSA disks retained the HSA, thus, enabling the separation of Cu-Cp and Cu-LMM species on the DEAE disk. First, one α-HSA disk was placed in front of one DEAE disk, applying a flow rate of 1 mL min^{-1} and 0.6 mL min^{-1}, but the HSA was not retained. Then, the flow rate was lowered to 0.3 mL min^{-1} and one more α-HSA disk was added. Applying these chromatographic conditions for

3 min, the HSA was quantitatively retained by the α-HSA disks. In order not to overload the α-HSA disks (disk capacity 0.87 mg mL^{-1} HSA support), 20 µL of 15-times diluted sample was injected.

It was found experimentally that under the same chromatographic conditions as previously used to separate the serum proteins on the DEAE disk, the HSA was retained on the α-HSA disks, while the Cp quantitatively passed the α-HSA disks and was separated on the DEAE disk. Then, the procedure was further optimized to elute the HSA retained on the α-HSA disks. Among the various eluents tested, i.e., 0.1, 0.5 and 1 mol L^{-1} glycine (pH 2.7), 0.1 mol L^{-1} citric acid (pH 3), 0.15 mol L^{-1} NH_4OH (pH 10.5), 0.5 mol L^{-1} arginine (pH 4.4) and 0.5 mol L^{-1} acetic acid, the last of these was selected since it quantitatively eluted the Cu-HSA from the CLC column at a flow rate of 1.0 mL min^{-1}. In addition to Cu-Cp and Cu-HSA, a small portion of serum Cu can also be associated with the LMM species, e.g., amino acids [92]. To verify whether the developed chromatographic procedure also enables the separation of the Cu-LMM species, a synthetic solution of the Cu-glycine was prepared (Cu to glycine ratio 1:100). Glycine was selected since it is among the most abundant amino acids present in human serum [144].

Chromatograms of the separation of the 15-times diluted sample of HSA (25 g L^{-1}) monitored by UV at 278 nm, and ICP-MS detection at m/z 63 and quantification of Cu-HSA by post-column ID-ICP-MS are presented in Figures 13 and 14, respectively.

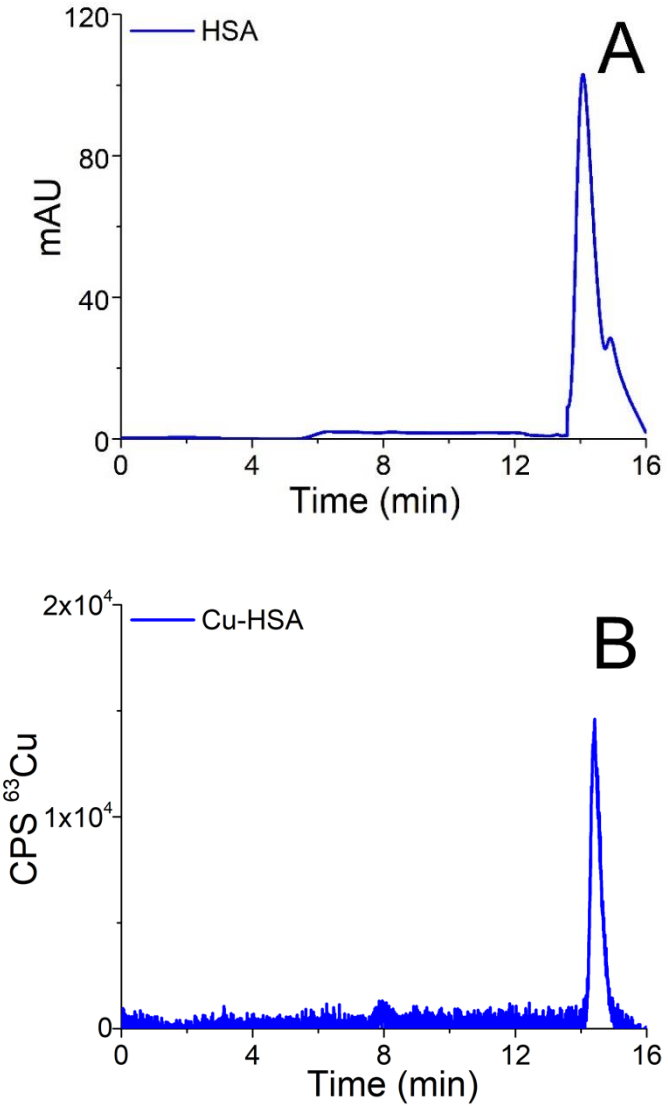

Figure 13: Chromatograms of separation of 15-times diluted sample of standard serum protein HSA (25 g L^{-1}) on the CLC monolithic column monitored by (A) UV detection at 278 nm and (B) ICP-MS detection at m/z 63.

The data in Figure 13 show that under optimized chromatographic conditions the HSA withstands the gradient elution with NH_4Cl and is retained by the α-HSA disks. Finally, the HSA is eluted from the α-HSA disks with acetic acid at elution times from 14.0 to 15.2 min. It is further seen that the elution of the HSA detected by UV takes place at the same elution time as the Cu detected by ICP-MS.

To verify whether the developed speciation procedure allows for the quantitative elution of Cu-HSA from the CLC column, the concentration of the eluted Cu was calculated by post-column ID-ICP-MS (the Cu mass flow used for the quantification is shown in Figure 14 and compared with the total Cu concentration injected.

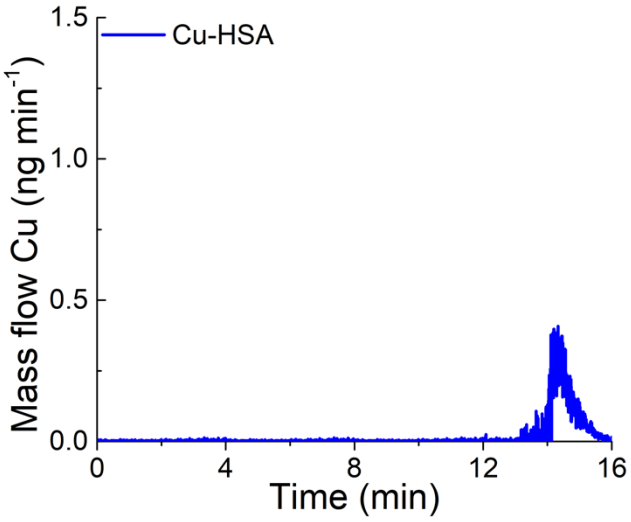

Figure 14: Chromatogram of separation of 15-times diluted sample of standard serum protein HSA (25 g L^{-1}) on the CLC monolithic column monitored by ICP-MS detection. Cu mass flow is based on measurements of isotope ratios m/z 63 and 65.

The Cu concentration eluted was found to be 146.1 ng mL^{-1}, while the total Cu was 152.2 ng mL^{-1}, indicating 96% column recovery. Thus, the Cu-HSA was quantitatively eluted from the column.

Chromatograms of the separation of the 15-times diluted samples of Cp (3g L^{-1}) on the CLC monolithic column monitored by UV at 278 nm, and ICP-MS detection at m/z 63 and quantification of Cu-Cp by post-column ID-ICP-MS are presented in Figures 15 and 16, respectively.

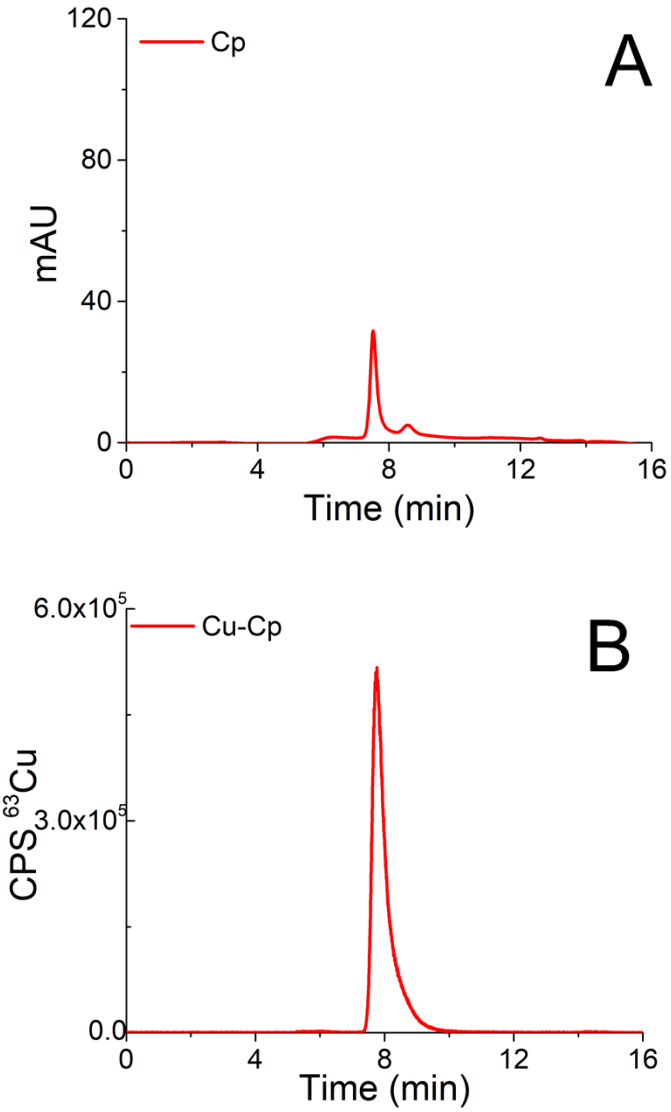

Figure 15: Chromatograms of separation of 15-times diluted sample of standard serum protein Cp (3 g L^{-1}) on the CLC monolithic column monitored by (A) UV detection at 278 nm and (B) ICP-MS detection at m/z 63.

The data in Figure 15 demonstrate that the Cp passes the α-HSA disks and is separated on the DEAE disk by gradient elution with NH_4Cl at elution times from 7.3 to 9.5 min. It can also be seen that it is well separated from the Cu-HSA (see Figures 13 and 14). It is evident that the elution of the Cp detected by UV takes place at the same elution time as the Cu detected by the ICP-MS.

To evaluate the efficiency of the Cu-Cp elution from the CLC column, the concentration of eluted Cu (calculated by post-column ID-ICP-MS) was compared with the total Cu concentration injected. The Cu mass flow used for the quantification is shown in Figure 16.

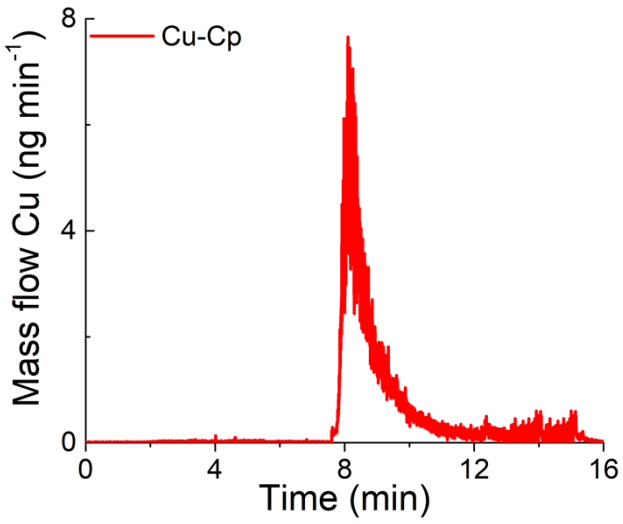

Figure 16: Chromatogram of separation of 15-times diluted sample of standard serum protein Cp (3 g L^{-1}) on the CLC monolithic column monitored by ICP-MS detection. Cu mass flow is based on measurements of isotope ratios m/z 63 and 65.

The Cu concentration eluted was found to be 423.5 ng mL^{-1}, while the total Cu was 439.0 ng mL^{-1}, indicating 97% column recovery. Hence, the Cu-Cp was quantitatively eluted from the column.

Chromatograms of the separation of Cu-glycine (47.0 ng mL^{-1} Cu) on the CLC monolithic column monitored by ICP-MS detection at m/z 63 and quantification of Cu-glycine by post-column ID-ICP-MS are presented in Figures 17 and 18, respectively (the UV signal of glycine is too weak, so it is not shown in Figure 17).

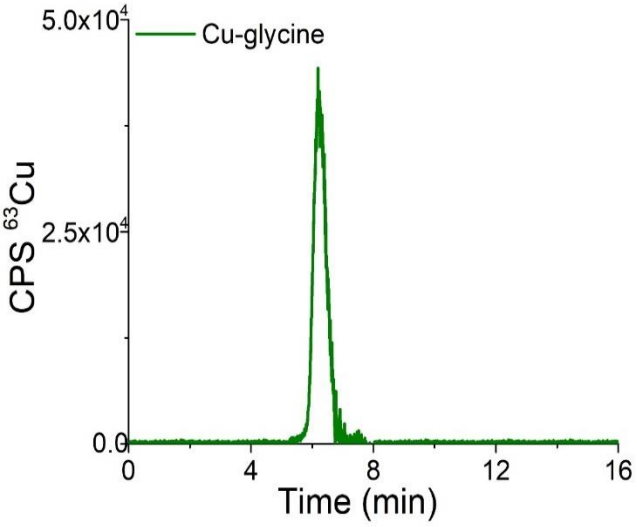

Figure 17: Chromatogram of separation of synthetically prepared Cu-glycine (47.0 ng L^{-1} Cu) on the CLC monolithic column monitored by ICP-MS detection at m/z 63.

As can be seen from Figure 17, the Cu-glycine is eluted from 5.6 to 6.9 min and is separated from the Cu-Cp (elution time from 7.3 to 9.5 min, Figure 15 and 16).

To evaluate the efficiency of the Cu-glycine elution from the CLC column, the concentration of eluted Cu (calculated by post-column ID-ICP-MS) was compared with the total Cu concentration injected. The Cu mass flow used for the quantification is shown in Figure 18.

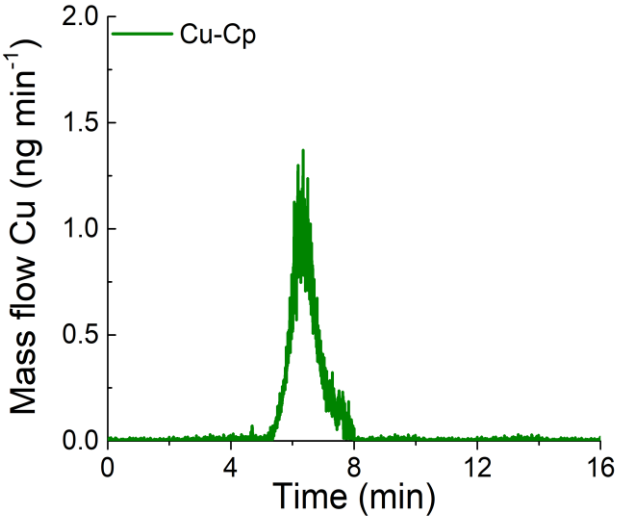

Figure 18: Chromatogram of separation of synthetically prepared Cu-glycine (47.0 ng mL^{-1} Cu) on the CLC monolithic column monitored by ICP-MS detection. Cu mass flow is based on measurements of isotope ratios m/z 63 and 65.

From the Cu concentration eluted from the column (47.5 ng mL^{-1}), determined by post-column ID-ICP-MS, and total Cu concentration (47.0 ng mL^{-1}) it is evident that the Cu-Cp is quantitatively eluted (column recovery 101%).

Based on the data presented in Figures 13-18 and the overall optimization of the analytical procedure, it can be concluded that the developed method enables the separation of Cu-glycine, Cu-Cp and Cu-HSA, and their quantitative elution from the CLC monolithic column, which extends its use to the determination of the Cu species in human serum.

Finally, the developed CLC-ID-ICP-MS method was applied for Cu speciation in human serum samples. Representative chromatograms of the 15-times diluted serum samples of two healthy individuals (samples H5 and H1) separated on the CLC column, monitored by ICP-MS detection at m/z 63, are presented in Figure 19. Due to the low Cp concentration in human serum (0.2 to 0.35 g L^{-1}) [145] and high sample dilution, it was not possible to follow the Cp elution profile by UV detection.

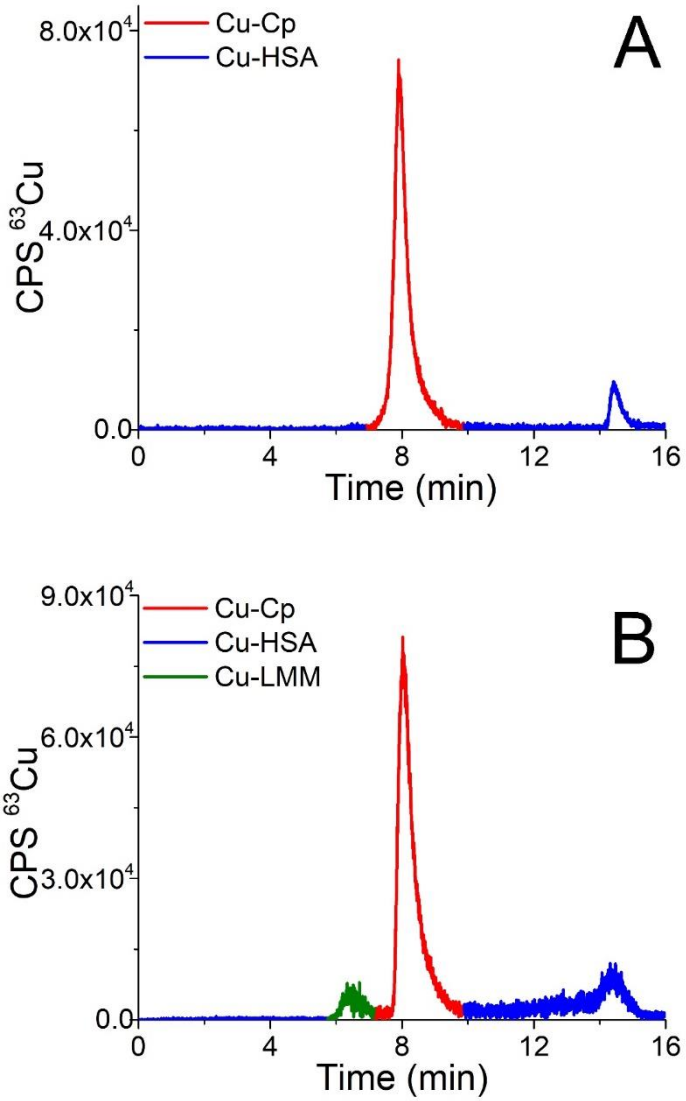

Figure 19: Chromatograms of separation of 15-times diluted human serum samples (A) H5 and (B) H1 on the CLC monolithic column monitored by ICP-MS detection at m/z 63.

The elution profile of Cu in Figure 19A (sample H5) shows that the Cu-Cp was eluted from 7.3 to 9.5 min and the Cu-HSA from 14.0 to 15.2 min, whereas in Figure 19B (sample H1) the fraction eluted from 5.6 to 6.9 min in front of the Cu-Cp peak is also noticeable. It most probably corresponds to Cu-LMM species, which might also be present in human serum [92].The Cu from the reagent blank contributed less than 1% to the background below the Cu-Cp peak in ICP-MS measurements.

The Cu species in human serum were quantified by post-column ID-ICP-MS analysis. A representative chromatogram of the mass flow (sample H1) is shown in Figure 20.

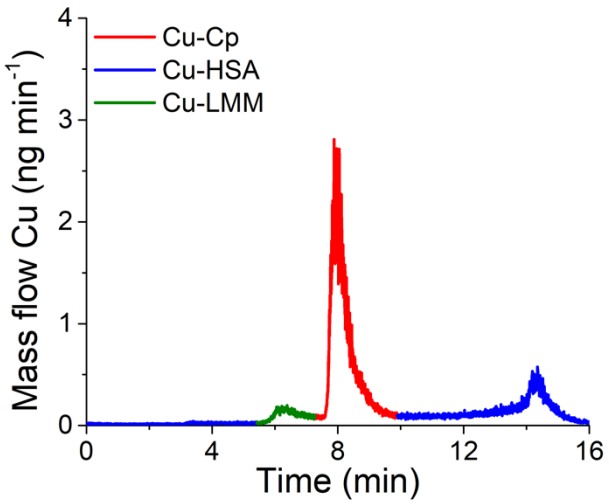

Figure 20: Chromatogram of separation of Cu species in 15-times diluted human serum sample H1 on the CLC monolithic column. Cu mass flow is based on measurements of isotope ratios *m/z* 63 and 65.

4.2.2 Analytical figures of merit

4.2.2.1 Resolution of the CLC column

The ability of the developed analytical method to separate Cu-LMM from Cu-Cp and Cu-Cp from Cu-HSA peaks was evaluated with a calculation of the resolution (R_S) of the CLC column, using Eq. 1 [146],

$$R_S = \frac{t_{R2} - t_{R1}}{0.5\,(W_1 + W_2)} \qquad \text{Eq. 2}$$

where t_{R1} and t_{R2} are the retention times of the first and second peaks, respectively, while W_1 and W_2 are their widths (expressed in time units). According to this equation, the two peaks are separated and can be quantified if the R_S value is equal to or higher than 1. The calculated R_S values for the Cu-LMM and Cu-Cp, and Cu-Cp and Cu-HSA peaks were 1.03 and 3.79, respectively, confirming that the peaks are well resolved.

4.2.2.2 Column recoveries

The column recoveries were verified by analyzing representative serum samples of the healthy individuals, the transplanted renal patients and the cancer patients. For this purpose, speciation analysis was applied to the 15-times diluted human serum samples. The column recoveries were calculated as the ratio between the Cu concentration eluted from the column (sum of Cu-LMM, Cu-Cp and Cu-HSA concentrations) and the total Cu concentrations in serum samples injected into the column. The results are summarized in Table 8.

Table 8: Column recoveries of the CLC-ID-ICP-MS procedure, calculated as the ratio between the sum of Cu species in human serum samples eluted from the CLC column and total Cu concentrations in serum samples injected.

Human serum sample	Total Cu (ng mL^{-1})	Cu-LMM (ng mL^{-1})	Cu-Cp (ng mL^{-1})	Cu-HSA (ng mL^{-1})	Sum of Cu species eluted (ng mL^{-1})	Column recovery (%)
H4	972 ± 4	62 ± 6	810 ± 8	107 ± 7	979 ± 10	101
T2	987 ± 3	< 3.3	870 ± 9	90.4 ± 5.4	960 ± 10	97
C3	1215 ± 15	39 ± 3	1127 ± 11	114 ± 7	1280 ± 15	105

H – Healthy individual
T – Transplanted renal patient
C – Cancer patient

The data from Table 1 indicate that the separated Cu species in the human serum were quantitatively eluted from the CLC column. The column recoveries ranged between 97 and 105%.

4.2.2.3 Repeatability of measurements, limits of detection, limits of quantification and linearity of measurement

The repeatability of the measurements was checked with six consecutive speciation analyses of human serum from a healthy individual. The data are given in Table 9.

Table 9: Repeatability of measurement for Cu speciation in human serum sample H1, LODs and LOQs applying CLC-ID-ICP-MS procedure.

Cu species	RSD (%)	LOD (ng mL^{-1} Cu)	LOQ (ng mL^{-1} Cu)
Cu-LMM	9.0	3.3	11
Cu-Cp	1.0	6.3	21
Cu-HSA	6.3	5.3	18

Good repeatability of the measurements was obtained for Cu-Cp. The relative standard deviation (RSD) between consecutive separations for the separated Cu-Cp was ± 1%. Slightly worse were the RSDs for the Cu-HSA (± 6.3%) and Cu-LMM species (± 9.0%) since their concentrations in the serum samples were significantly lower than that of the Cu-Cp.

The limits of detection (LODs) and the limits of quantification (LOQs) for the determination of the separated Cu species were calculated as the concentrations that provide signals (peak areas) equal to $3s$ and $10s$ of a blank sample (buffer A) in the chromatogram, respectively. The LODs and LOQs were calculated on the basis of six blank samples injected into the CLC monolithic column, considering the same dilution factor (15-times) as in the analysis of the serum samples. The data for the LODs and LOQs are presented in Table 9. The LODs and LOQs for the separated Cu species ranged from 3.3 to 6.3 ng mL^{-1} Cu and 11 to 21 ng mL^{-1} Cu, respectively. These LOQs are low enough to perform Cu speciation analyses in human serum samples.

The linearity of the measurement for the separated Cr species was confirmed over the concentration range from LOQ to 500 ng mL^{-1} Cu, with a correlation coefficient (R^2) better than 0.997.

4.2.2.4 Accuracy of the determination of Cu species concentrations in human serum using the CLC-ID-ICP-MS procedure and the total Cu concentration in serum using ICP-MS

Since there are no certified reference materials available for the Cu-Cp, Cu-HSA and Cu-LMM species, the accuracy of the determination of the Cu species concentrations in serum samples was checked using the CLC-ID-ICP-MS procedure.

The accuracy of the determination of the total Cu concentration in serum was tested by analyzing the Seronorm Level 1 quality control material. The determined Cu concentration (1074 ± 9 ng mL^{-1}) agreed well with the certified value (1088 ± 89 ng mL^{-1}), confirming the accuracy of the analytical procedure.

The main advantage of the newly developed CLC-ID-ICP-MS method, which combines immunoaffinity and anion-exchange chromatography over previously reported ones, is its simplicity and ability to perform rapid 2D separation (16 min) and reliable quantification of the Cu species (Cu-Cp, Cu-HSA and Cu-LMM) in human serum in a single chromatographic run. Other researchers reported the determination of Cu-Cp only, applying 2D separation in two chromatographic runs [127], the determination of Cu-Cp and Cu-HSA on anion-exchange chromatographic columns [33], [34] or exchangeable Cu in human serum [130].

4.2.3 Speciation of Cu in human serum

The developed and validated CLC-ID-ICP-MS method for the speciation of Cu in human serum was applied to the analysis of human serum samples from six healthy individuals (samples H1-H6), four transplanted renal patients (samples T1-T4) and six lung cancer patients (samples C1-C6).

The distribution of the Cu concentrations between the Cu-Cp, Cu-HSA and Cu-LMM species in the serum samples separated on the CLC column and quantified by post-column ID-ICP-MS, and the total Cu concentrations determined by ICP-MS is shown in Figure 21.

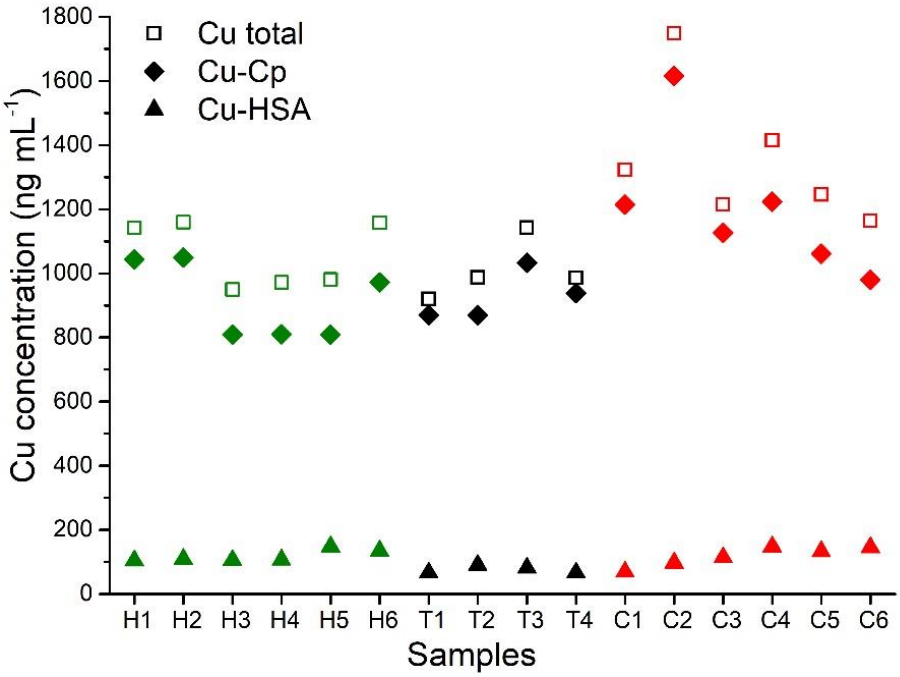

Figure 21: Distribution of Cu concentrations between Cu-Cp, Cu-HSA and Cu-LMM species in human serum samples separated on a CLC column and quantified by post-column ID-ICP-MS, and the total Cu concentrations determined by ICP-MS in healthy individuals (H), transplanted renal patients (T) and cancer patients (C).

The Cu concentrations related to the data from Figure 21 are provided in Table 10.

Table 10: Total Cu concentrations in the serum of healthy individuals, transplanted renal patients and cancer patients determined by ICP-MS, and concentrations of Cu-LMM, Cu-Cp and Cu-HSA determined by the CLC-ID-ICP-MS procedure n=2 (for each sample, values of 2 independent measurements are provided).[a]

Sample	Total Cu ($ng\ mL^{-1}$)	Cu-LMM ($ng\ mL^{-1}$)	Cu-Cp ($ng\ mL^{-1}$)	Cu-HSA ($ng\ mL^{-1}$)	$\sum$ of Cu species ($ng\ mL^{-1}$)
H1	1147	59.0	1051	109	1219
	1138	52.0	1035	98.0	1185
H2	1168	69.8	1055	116	1241
	1153	57.5	1044	104	1206
H3	961	<3.3	816	111	927
	939	<3.3	804	98.0	902
H4	974	58.0	816	112	986
	969	66.0	804	102	972
H5	984	<3.3	815	154	969
	978	<3.3	802	142	944
H6	1160	<3.3	979	141	1120
	1155	<3.3	965	130	1095
T1	925	<3.3	887	69.0	956
	916	<3.3	874	62.2	936
T2	990	<3.3	864	94.0	958
	984	<3.3	877	87.0	964
T3	1149	<3.3	1039	85.0	1124
	1137	<3.3	1027	77.0	1104
T4	992	<3.3	961	69.0	1030
	979	<3.3	948	63.0	1011
C1	1329	<3.3	1223	73.05	1296
	1317	<3.3	1205	65.0	1270
C2	1760	<3.3	1628	103	1731
	1736	<3.3	1604	92.4	1696
C3	1226	41.0	1118	119	1278
	1205	37.0	1135	109	1281
C4	1419	51.0	1232	155	1438
	1411	43.0	1215	138	1396
C5	1253	65.0	1068	138	1271
	1238	53.0	1054	127	1234
C6	1168	64.0	987	151	1202
	1157	53.0	972	139	1164

[a]H-healthy individual; T- transplanted renal patient; C-cancer patient

The data from Figure 21 indicate that concentrations of the Cu-Cp and those of the total Cu are in general higher in the serum samples of the cancer and transplanted renal patients than in the healthy individuals. Furthermore, it is evident that the Cu-HSA

concentrations are generally lower in the transplanted renal patients. In 7 out of the 20 serum samples analyzed, the Cu-LMM species were also identified.

In assessing the possible statistical significance of the differences between the population of healthy individuals and the population of cancer or renal patients, the H1 and H2 samples were excluded from the calculations in the healthy population due to recent recovery from viral infection. The mean values between the Cu-Cp, Cu-HSA and total Cu were compared for individual Cu species by computing Student's *t*-test for the population of cancer patients (n = 6) and healthy individuals (n = 4), or transplanted renal patients (n = 4) and healthy individuals (n = 4).

Higher concentrations of Cu-Cp and total Cu were observed in the cancer patients' group in comparison to the healthy individuals, while the Cu-HSA concentrations were similar. Significant differences ($p < 0.05$) between the two populations were obtained for Cu-Cp and total Cu. The Cu-Cp was found as the most distinctive species ($p = 0.0093$), while the p value for total Cu ($p = 0.0117$) differed less. There was no statistical difference observed for Cu-HSA between the populations of cancer patients and healthy individuals ($p = 0.979$). These observations showed the potential of Cu-Cp as a possible biomarker for cancer diagnosis. Cp has already been proposed as a prognostic biomarker in breast, bladder, and bile duct cancer [113]–[115] and a candidate marker for ovarian clear cell carcinoma [116].

Lower concentrations of Cu-HSA, and slightly higher concentrations of Cu-Cp and total Cu, were observed in the group of transplanted renal patients compared to the healthy individuals. Significant differences between the two populations were found for Cu-HSA ($p = 0.0011$), while there was no statistical difference observed for Cu-Cp and total Cu ($p = 0.1783$ and 0.9251, respectively). The lower Cu-HSA concentrations obtained are consistent with hypo-albuminemia, which is common in patients with end-stage renal disease [147].

Chapter 5

Conclusions

In this doctoral study an analytical method for the speciation analysis of Ru-based candidate drugs was optimized, and the kinetics of the interaction of the drugs with the main human serum proteins was studied. A new analytical method was also developed for the reliable determination of Cu species in human serum.

The CLC monolithic column assembled from one affinity CIM Protein G and one weak anion-exchange CIM DEAE disk was used for the separation of the Ru complexes [(η6-p-cymene)Ru(1-hydroxypyridine-2(1H)-thionato)Cl] **(1)** and [(η6-p-cymene)Ru(1-hydroxypyridine-2(1H)-thionato)pta]PF6 **(2)** in human serum. The separated Ru species were monitored on-line by UV spectrometry at 278 nm and ICP-MS at m/z 99 and 101. The post-column ID-ICP-MS performed accurate quantification of the separated Ru species. The method is selective, robust, repeatable, reproducible (RSD for separated chloride **(1)** and Ru species <4 and 7%, respectively), of sufficient sensitivity (LODs and LOQs for separated Ru species <1.6 and 5.3 ng mL^{-1} Ru, respectively), and demonstrated its potential for studies of the kinetics of bindings of Ru complexes **(1)** and **(2)** with human serum proteins. The data revealed that both Ru complexes interacted mainly with HSA. Complex **(1)** more rapidly and to a greater extent bind to HSA than complex **(2)**. The equilibrium concentration, in which around 70% of complex **(1)** is bound to HSA, 5% is associated with IgG and the other 25% remains as a free drug, was reached 6 h after incubation. The interaction of complex **(2)** with HSA was much slower and less extensive than with complex **(1)**. The equilibrium concentration was obtained 24 h after incubation, with about 50% of complex **(2)** bound to HSA, while 50% of complex (**2**) remained unbound. This detailed study on the binding kinetics of **(1)** and **(2)** suggests that bound and unbound forms of the complexes are present in human serum, which is an important finding for drug design, where pharmacokinetics, as well as pharmacodynamics properties, must be well defined.

A novel analytical method for the speciation of Cu in human serum based on CLC monolithic chromatography with post-column ID-ICP-MS detection was developed. 2D separation of the Cu species was achieved in a single chromatographic run on a column constructed by assembling two immunoaffinity CIMmic α-HSA disks and one CIMmic weak anion-exchange DEAE disk into a single housing. Post-column ID-ICP-MS quantified the separated Cu species. During separation, the HSA was first retained on the α-HSA disks, enabling the separation of Cu-LMM species from Cu-Cp using NH_4Cl (pH 7.4) as an eluent. The elution with acetic acid that followed allowed further separation of the Cu-HSA. The developed method enables quantitative and reliable determinations of the Cu-Cp, Cu-HSA and a fraction that most probably corresponds to the Cu-LMM species in human serum. The previously reported analytical procedures are limited to a determination of the exchangeable Cu or enable the determination of Cu-Cp, or Cu-Cp and Cu-HSA, but

cannot quantify the Cu-LMM species. A statistical evaluation of the results (Student's *t*-test) revealed that the total Cu and Cu-Cp concentrations were higher in the population of cancer patients than in the population of healthy individuals, with Cu-Cp being the most differentiating species. This confirms that Cu-Cp is a potential biomarker in cancer diagnosis. The results also showed that the Cu-HSA concentrations were lower in transplanted renal patients, which is consistent with the usually lower HSA levels in this patient population. Our research provides an important, new analytical tool that can be used to assess Cu metabolic disorders in many other diseases.

Finally, the outcomes from the doctoral research will contribute to developing advanced and reliable analytical methods in the growing research field of speciation analysis and metallomics.

References

[1] D. M. Templeton, F. Ariese, R. Cornelis, L.-G. Danielsson, H. Muntau, and H. P. V. Leeuwen, "(IUPAC Recommendations 2000)," *Pure and Applied Chemistry*, p. 18, 2000.

[2] W. Quiroz, "Speciation analysis in chemistry," *ChemTexts*, vol. 7, no. 1, p. 7, Mar. 2021, doi: 10.1007/s40828-020-00125-8.

[3] A. N. Paiva *et al.*, "Beneficial effects of oral chromium picolinate supplementation on glycemic control in patients with type 2 diabetes: A randomized clinical study," *Journal of Trace Elements in Medicine and Biology*, vol. 32, pp. 66–72, Oct. 2015, doi: 10.1016/j.jtemb.2015.05.006.

[4] R. R. Ray, "Review article. Adverse hematological effects of hexavalent chromium: an overview," *Interdisciplinary Toxicology*, vol. 9, no. 2, pp. 55–65, Jun. 2016, doi: 10.1515/intox-2016-0007.

[5] Sandra Mounicou, J. Szpunar, and R. Lobinski, "Metallomics: the concept and methodology," *Chem. Soc. Rev.*, pp. 1119–1138, Jul. 2009, doi: 10.1039/b713633c.

[6] R. A. Yokel, S. M. Lasley, and D. C. Dorman, "The Speciation of Metals in Mammals Influences Their Toxicokinetics and Toxicodynamics and Therefore Human Health Risk Assessment [1]," *Journal of Toxicology and Environmental Health, Part B*, vol. 9, no. 1, pp. 63–85, Jan. 2006, doi: 10.1080/15287390500196230.

[7] K. A. Lawton *et al.*, "Analysis of the adult human plasma metabolome," p. 15, 2008.

[8] N. L. Anderson, "The Clinical Plasma Proteome: A Survey of Clinical Assays for Proteins in Plasma and Serum," *Clinical Chemistry*, vol. 56, no. 2, pp. 177–185, Feb. 2010, doi: 10.1373/clinchem.2009.126706.

[9] J. Gailer, "Improving the safety of metal-based drugs by tuning their metabolism with chemoprotective agents," *Journal of Inorganic Biochemistry*, vol. 179, pp. 154–157, Feb. 2018, doi: 10.1016/j.jinorgbio.2017.11.008.

[10] K. A. Doucette, K. N. Hassell, and D. C. Crans, "Selective speciation improves efficacy and lowers toxicity of platinum anticancer and vanadium antidiabetic drugs," *Journal of Inorganic Biochemistry*, vol. 165, pp. 56–70, Dec. 2016, doi: 10.1016/j.jinorgbio.2016.09.013.

[11] H. U. Holtkamp and C. G. Hartinger, "Advanced metallomics methods in anticancer metallodrug mode of action studies," *TrAC Trends in Analytical Chemistry*, vol. 104, pp. 110–117, Jul. 2018, doi: 10.1016/j.trac.2017.09.023.

[12] L. Galvez *et al.*, "Critical assessment of different methods for quantitative measurement of metallodrug-protein associations," *Anal Bioanal Chem*, vol. 410, no. 27, pp. 7211–7220, Nov. 2018, doi: 10.1007/s00216-018-1328-8.

[13] M. Wenzel and A. Casini, "Mass spectrometry as a powerful tool to study therapeutic metallodrugs speciation mechanisms: Current frontiers and perspectives," *Coordination Chemistry Reviews*, vol. 352, pp. 432–460, Dec. 2017, doi: 10.1016/j.ccr.2017.02.012.

[14] A. Kot and J. Namiesnèik, "The role of speciation in analytical chemistry," *trends in analytical chemistry*, vol. 19, p. 11, 2000.

[15] J. Kladnik, J. Kljun, H. Burmeister, I. Ott, I. Romero-Canelón, and I. Turel, "Towards Identification of Essential Structural Elements of Organoruthenium(II)-Pyrithionato Complexes for Anticancer Activity," *Chem. Eur. J.*, vol. 25, no. 62, pp. 14169–14182, Nov. 2019, doi: 10.1002/chem.201903109.

[16] J. M. Walshe, "Wilson's disease: the importance of measuring serum caeruloplasmin non-immunologically," *Ann Clin Biochem*, vol. 40, no. 2, pp. 115–121, Mar. 2003, doi: 10.1258/000456303763046021.

[17] B. Michalke, *Metallomics: Analytical Techniques and Speciation Methods*. Wiley, 2016. [Online]. Available: https://books.google.si/books?id=FN0QDQAAQBAJ

[18] J. García-Bellido, L. Freije-Carrelo, M. Moldovan, and J. R. Encinar, "Recent advances in GC-ICP-MS: Focus on the current and future impact of MS/MS technology," *TrAC Trends in Analytical Chemistry*, vol. 130, p. 115963, Sep. 2020, doi: 10.1016/j.trac.2020.115963.

[19] H. Rekhi, S. Rani, N. Sharma, and A. K. Malik, "A Review on Recent Applications of High-Performance Liquid Chromatography in Metal Determination and Speciation Analysis," *Critical Reviews in Analytical Chemistry*, vol. 47, no. 6, pp. 524–537, Nov. 2017, doi: 10.1080/10408347.2017.1343659.

[20] B. Michalke, D. Willkommen, and V. Venkataramani, "Iron Redox Speciation Analysis Using Capillary Electrophoresis Coupled to Inductively Coupled Plasma Mass Spectrometry (CE-ICP-MS)," *Front. Chem.*, vol. 7, p. 136, Mar. 2019, doi: 10.3389/fchem.2019.00136.

[21] L. Hu *et al.*, "Identification of Metal-Associated Proteins in Cells by Using Continuous-Flow Gel Electrophoresis and Inductively Coupled Plasma Mass Spectrometry," *Angew. Chem. Int. Ed.*, vol. 52, no. 18, pp. 4916–4920, Apr. 2013, doi: 10.1002/anie.201300794.

[22] R. Łobiński, D. Schaumlöffel, and J. Szpunar, "Mass spectrometry in bioinorganic analytical chemistry," *Mass Spectrom. Rev.*, vol. 25, no. 2, pp. 255–289, Mar. 2006, doi: 10.1002/mas.20069.

[23] T. Hasegawa, Y. Wakita, Y. Zhu, H. Matsuura, H. Haraguchi, and T. Umemura, "Speciation of Human Serum Proteins Based on Trace Metal Mapping Analysis by CIM Monolithic Disk Column HPLC/ICP-MS in Complement with Off-Line MALDI-TOF-MS Analysis," *BCSJ*, vol. 80, no. 3, pp. 503–506, Mar. 2007, doi: 10.1246/bcsj.80.503.

[24] A. L. Rosen and G. M. Hieftje, "Inductively coupled plasma mass spectrometry and electrospray mass spectrometry for speciation analysis: applications and instrumentation," *Spectrochimica Acta Part B: Atomic Spectroscopy*, vol. 59, no. 2, pp. 135–146, Feb. 2004, doi: 10.1016/j.sab.2003.09.004.

[25] A. Gonzalvez, M. L. Cervera, S. Armenta, and M. de la Guardia, "A review of non-chromatographic methods for speciation analysis," *Analytica Chimica Acta*, vol. 636, no. 2, pp. 129–157, Mar. 2009, doi: 10.1016/j.aca.2009.01.065.

[26] J. Szpunar, R. \Lobiński, and R. M. Smith, *Hyphenated Techniques in Speciation Analysis*. Royal Society of Chemistry, 2003. [Online]. Available: https://books.google.si/books?id=AvN_oVerKsEC

[27] S. Hann *et al.*, "Application of HPLC-ICP-MS to speciation of cisplatin and its degradation products in water containing different chloride concentrations and in human urine," *J. Anal. At. Spectrom.*, vol. 18, no. 11, pp. 1391–1395, 2003, doi: 10.1039/B309028K.

[28] S. Hann, Zs. Stefanka, K. Lenz, and G. Stingeder, "Novel separation method for highly sensitive speciation of cancerostatic platinum compounds by HPLC-ICP-MS," *Anal Bioanal Chem*, vol. 381, no. 2, pp. 405–412, Jan. 2005, doi: 10.1007/s00216-004-2839-z.

[29] P. Hemström, Y. Nygren, E. Björn, and K. Irgum, "Alternative organic solvents for HILIC separation of cisplatin species with on-line ICP-MS detection," *J. Sep. Sci.*, vol. 31, no. 4, pp. 599–603, Mar. 2008, doi: 10.1002/jssc.200700480.

[30] T. Falta, G. Koellensperger, A. Standler, W. Buchberger, R. M. Mader, and S. Hann, "Quantification of cisplatin, carboplatin and oxaliplatin in spiked human plasma samples by ICP-SFMS and hydrophilic interaction liquid chromatography (HILIC) combined with ICP-MS detection," *J. Anal. At. Spectrom.*, vol. 24, no. 10, p. 1336, 2009, doi: 10.1039/b907011g.

[31] K. Marković *et al.*, "Monolithic chromatography on conjoint liquid chromatography columns for speciation of platinum-based chemotherapeutics in serum of cancer patients," *Journal of Trace Elements in Medicine and Biology*, vol. 57, pp. 28–39, Jan. 2020, doi: 10.1016/j.jtemb.2019.09.011.

[32] A. Martincic, R. Milacic, M. Cemazar, G. Sersa, and J. Scancar, "The use of CIM-DEAE monolithic chromatography coupled to ICP-MS to study the distribution of cisplatin in human serum," *Anal. Methods*, vol. 4, no. 3, p. 780, 2012, doi: 10.1039/c2ay05603h.

[33] N. Solovyev, A. Ala, M. Schilsky, C. Mills, K. Willis, and C. F. Harrington, "Biomedical copper speciation in relation to Wilson's disease using strong anion exchange chromatography coupled to triple quadrupole inductively coupled plasma mass spectrometry," *Analytica Chimica Acta*, vol. 1098, pp. 27–36, Feb. 2020, doi: 10.1016/j.aca.2019.11.033.

[34] M. E. del Castillo Busto, S. Cuello-Nunez, C. Ward-Deitrich, T. Morley, and H. Goenaga-Infante, "A fit-for-purpose copper speciation method for the determination of exchangeable copper relevant to Wilson's disease," *Anal Bioanal Chem*, vol. 414, no. 1, pp. 561–573, Jan. 2022, doi: 10.1007/s00216-021-03517-y.

[35] A. Lothian and B. R. Roberts, "Standards for Quantitative Metalloproteomic Analysis Using Size Exclusion ICP-MS," *JoVE*, no. 110, p. 53737, Apr. 2016, doi: 10.3791/53737.

[36] M. H. M. Klose *et al.*, "Serum-binding properties of isosteric ruthenium and osmium anticancer agents elucidated by SEC–ICP–MS," *Monatsh Chem*, vol. 149, no. 10, pp. 1719–1726, Oct. 2018, doi: 10.1007/s00706-018-2280-1.

[37] S. Hann, T. Falta, K. Boeck, M. Sulyok, and G. Koellensperger, "On-line fast column switching SEC × IC separation combined with ICP-MS detection for mapping

metallodrug–biomolecule interaction," *J. Anal. At. Spectrom.*, vol. 25, no. 6, p. 861, 2010, doi: 10.1039/c000427h.

[38] D. Esteban-Fernández, E. Moreno-Gordaliza, B. Cañas, M. Antonia Palacios, and M. Milagros Gómez-Gómez, "Analytical methodologies for metallomics studies of antitumor Pt-containing drugs," *Metallomics*, vol. 2, no. 1, pp. 19–38, 2010, doi: 10.1039/B911438F.

[39] R. R.Burgess, "A brief practical review of size exclusion chromatography: Rules of thumb, limitations, and troubleshooting," *Protein Expression and Purification*, vol. 150, no. 1046–5928, pp. 81–85, Oct. 2018, doi: https://doi.org/10.1016/j.pep.2018.05.007.

[40] R. Milačič, T. Zuliani, J. Vidmar, and J. Ščančar, "Monolithic chromatography in speciation analysis of metal-containing biomolecules: a review," *J. Anal. At. Spectrom.*, vol. 31, no. 9, pp. 1766–1779, 2016, doi: 10.1039/C6JA00121A.

[41] J. Ščančar and R. Milačič, "Applications of methacrylate-based monolithic supports for speciation analysis," *J. Sep. Science*, vol. 32, no. 15–16, pp. 2495–2503, Aug. 2009, doi: 10.1002/jssc.200900219.

[42] A. Podgornik and N. L. Krajnc, "Application of monoliths for bioparticle isolation: Liquid Chromatography," *J. Sep. Science*, vol. 35, no. 22, pp. 3059–3072, Nov. 2012, doi: 10.1002/jssc.201200387.

[43] A. Podgornik, S. Yamamoto, M. Peterka, and N. L. Krajnc, "Fast separation of large biomolecules using short monolithic columns," *Journal of Chromatography B*, vol. 927, pp. 80–89, May 2013, doi: 10.1016/j.jchromb.2013.02.004.

[44] J. C. Masini and F. Svec, "Porous monoliths for on-line sample preparation: A review," *Analytica Chimica Acta*, vol. 964, pp. 24–44, Apr. 2017, doi: 10.1016/j.aca.2017.02.002.

[45] J. Ščančar and R. Milačič, "Monolithic chromatography for elemental and speciation analysis," *TrAC Trends in Analytical Chemistry*, vol. 28, no. 9, pp. 1048–1056, Oct. 2009, doi: 10.1016/j.trac.2009.06.005.

[46] A. Schmidt, H. Helgers, F. L. Vetter, A. Juckers, and J. Strube, "Fast and Flexible mRNA Vaccine Manufacturing as a Solution to Pandemic Situations by Adopting Chemical Engineering Good Practice—Continuous Autonomous Operation in Stainless Steel Equipment Concepts," *Processes*, vol. 9, no. 11, p. 1874, Oct. 2021, doi: 10.3390/pr9111874.

[47] M. Zhao, M. Vandersluis, J. Stout, U. Haupts, M. Sanders, and R. Jacquemart, "Affinity chromatography for vaccines manufacturing: Finally ready for prime time?," *Vaccine*, vol. 37, no. 36, pp. 5491–5503, Aug. 2019, doi: 10.1016/j.vaccine.2018.02.090.

[48] L. Zhao, Q. Zhu, L. Mao, Y. Chen, H. Lian, and X. Hu, "Preparation of thiol- and amine-bifunctionalized hybrid monolithic column via 'one-pot' and applications in speciation of inorganic arsenic," *Talanta*, vol. 192, pp. 339–346, Jan. 2019, doi: 10.1016/j.talanta.2018.09.064.

[49] X. Ou, C. Wang, M. He, B. Chen, and B. Hu, "Online simultaneous speciation of ultra-trace inorganic antimony and tellurium in environmental water by polymer monolithic capillary microextraction combined with inductively coupled plasma mass spectrometry," *Spectrochimica Acta Part B: Atomic Spectroscopy*, vol. 168, p. 105854, Jun. 2020, doi: 10.1016/j.sab.2020.105854.

[50] L. Zhao, J. Fei, H. Lian, L. Mao, and X. Cui, "Development of a novel amine- and carboxyl-bifunctionalized hybrid monolithic column for non-invasive speciation analysis of chromium," *Talanta*, vol. 212, p. 120799, May 2020, doi: 10.1016/j.talanta.2020.120799.

[51] R. Milačič, D. Ajlec, T. Zuliani, D. Žigon, and J. Ščančar, "Determination of Zn-citrate in human milk by CIM monolithic chromatography with atomic and mass spectrometry detection," *Talanta*, vol. 101, pp. 203–210, Nov. 2012, doi: 10.1016/j.talanta.2012.09.002.

[52] J. Ščančar, T. Zuliani, D. Žigon, and R. Milačič, "Ni speciation in tea infusions by monolithic chromatography—ICP-MS and Q-TOF-MS," *Anal Bioanal Chem*, vol. 405, no. 6, pp. 2041–2051, Feb. 2013, doi: 10.1007/s00216-012-6611-5.

[53] K. Peeters, T. Zuliani, D. Žigon, R. Milačič, and J. Ščančar, "Nickel speciation in cocoa infusions using monolithic chromatography – Post-column ID-ICP-MS and Q-TOF-MS," *Food Chemistry*, vol. 230, pp. 327–335, Sep. 2017, doi: 10.1016/j.foodchem.2017.03.050.

[54] S. Murko, R. Milačič, and J. Ščančar, "Speciation of Al in human serum by convective-interaction media fast-monolithic chromatography with inductively coupled plasma mass spectrometric detection," *Journal of Inorganic Biochemistry*, vol. 101, no. 9, pp. 1234–1241, Sep. 2007, doi: 10.1016/j.jinorgbio.2007.06.013.

[55] R. Larios, M. E. Del Castillo Busto, D. Garcia-Sar, C. Ward-Deitrich, and H. Goenaga-Infante, "Accurate quantification of carboplatin adducts with serum proteins by monolithic chromatography coupled to ICPMS with isotope dilution analysis," *J. Anal. At. Spectrom.*, vol. 34, no. 4, pp. 729–740, 2019, doi: 10.1039/C8JA00409A.

[56] S. Murko, R. Milačič, B. Kralj, and J. Ščančar, "Convective Interaction Media Monolithic Chromatography with ICPMS and Ultraperformance Liquid Chromatography−Electrospray Ionization MS Detection: A Powerful Tool for Speciation of Aluminum in Human Serum at Normal Concentration Levels," *Anal. Chem.*, vol. 81, no. 12, pp. 4929–4936, Jun. 2009, doi: 10.1021/ac9006232.

[57] M. Bergant, J. Ščančar, and R. Milačič, "Kinetics of interaction of Cr(VI) and Cr(III) with serum constituents and detection of Cr species in human serum at physiological concentration levels," *Talanta*, vol. 218, p. 121199, Oct. 2020, doi: 10.1016/j.talanta.2020.121199.

[58] A. Martinčič, M. Cemazar, G. Sersa, V. Kovač, R. Milačič, and J. Ščančar, "A novel method for speciation of Pt in human serum incubated with cisplatin, oxaliplatin and carboplatin by conjoint liquid chromatography on monolithic disks with UV and ICP-MS detection," *Talanta*, vol. 116, pp. 141–148, Nov. 2013, doi: 10.1016/j.talanta.2013.05.016.

[59] A. Martinčič, R. Milačič, J. Vidmar, I. Turel, B. K. Keppler, and J. Ščančar, "New method for the speciation of ruthenium-based chemotherapeutics in human serum by conjoint liquid chromatography on affinity and anion-exchange monolithic disks," *Journal of Chromatography A*, vol. 1371, pp. 168–176, Dec. 2014, doi: 10.1016/j.chroma.2014.10.054.

[60] WHO, "WHO data." 2022. [Online]. Available: https://www.who.int/news-room/fact-sheets/detail/cancer

[61] H. Sung *et al.*, "Global Cancer Statistics 2020: GLOBOCAN Estimates of Incidence and Mortality Worldwide for 36 Cancers in 185 Countries," *CA A Cancer J Clin*, vol. 71, no. 3, pp. 209–249, May 2021, doi: 10.3322/caac.21660.

[62] T. Dyba *et al.*, "The European cancer burden in 2020: Incidence and mortality estimates for 40 countries and 25 major cancers," *European Journal of Cancer*, vol. 157, pp. 308–347, Nov. 2021, doi: 10.1016/j.ejca.2021.07.039.

[63] P. S. Moore and Y. Chang, "Why do viruses cause cancer? Highlights of the first century of human tumour virology," *Nat Rev Cancer*, vol. 10, no. 12, pp. 878–889, Dec. 2010, doi: 10.1038/nrc2961.

[64] D. B. Polk and R. M. Peek, "Helicobacter pylori: gastric cancer and beyond," *Nat Rev Cancer*, vol. 10, no. 6, pp. 403–414, Jun. 2010, doi: 10.1038/nrc2857.

[65] H. Jayatilaka *et al.*, "Tumor cell density regulates matrix metalloproteinases for enhanced migration," *Oncotarget*, vol. 9, no. 66, pp. 32556–32569, Aug. 2018, doi: 10.18632/oncotarget.25863.

[66] J. A. Nagy, S.-H. Chang, A. M. Dvorak, and H. F. Dvorak, "Why are tumour blood vessels abnormal and why is it important to know?," *Br J Cancer*, vol. 100, no. 6, pp. 865–869, Mar. 2009, doi: 10.1038/sj.bjc.6604929.

[67] D. Hanahan, "Hallmarks of Cancer: New Dimensions," *Cancer Discovery*, vol. 12, no. 1, pp. 31–46, Jan. 2022, doi: 10.1158/2159-8290.CD-21-1059.

[68] P. Anand *et al.*, "Cancer is a Preventable Disease that Requires Major Lifestyle Changes," *Pharm Res*, vol. 25, no. 9, pp. 2097–2116, Sep. 2008, doi: 10.1007/s11095-008-9661-9.

[69] P. Blinman, M. King, R. Norman, R. Viney, and M. R. Stockler, "Preferences for cancer treatments: an overview of methods and applications in oncology," *Annals of Oncology*, vol. 23, no. 5, pp. 1104–1110, May 2012, doi: 10.1093/annonc/mdr559.

[70] A. Pearce *et al.*, "Incidence and severity of self-reported chemotherapy side effects in routine care: A prospective cohort study," *PLoS ONE*, vol. 12, no. 10, p. e0184360, Oct. 2017, doi: 10.1371/journal.pone.0184360.

[71] M. T. Amjad, A. Chidharla, and A. Kasi, *Cancer Chemotherapy*. StatPearls Publishing, Treasure Island (FL), 2022. [Online]. Available: https://www.ncbi.nlm.nih.gov/books/NBK564367/

[72] L. Falzone, S. Salomone, and M. Libra, "Evolution of Cancer Pharmacological Treatments at the Turn of the Third Millennium," *Front. Pharmacol.*, vol. 9, p. 1300, Nov. 2018, doi: 10.3389/fphar.2018.01300.

[73] B. G. Katzung, Ed., *Basic & clinical pharmacology*, Fourteenth edition. New York Chicago San Francisco Athens London Madrid Mexico City Milan New Delhi Singapore Sydney Toronto: McGraw-Hill Education, 2018.

[74] M. Rowland and T. N. Tozer, *Clinical pharmacokinetics and pharmacodynamics: concepts and applications*, 4th ed. Philadelphia: Wolters Kluwer health - Lippincott William & Wilkins, 2011.

[75] J.-S. Kang and M.-H. Lee, "Overview of Therapeutic Drug Monitoring," *Korean J Intern Med*, vol. 24, no. 1, p. 1, 2009, doi: 10.3904/kjim.2009.24.1.1.

[76] A. Di Paolo and G. Bocci, "Drug distribution in tumors: Mechanisms, role in drug resistance, and methods for modification," *Curr Oncol Rep*, vol. 9, no. 2, pp. 109–114, Jan. 2007, doi: 10.1007/s11912-007-0006-3.

[77] S. T. Stern, M. N. Martinez, and D. M. Stevens, "When Is It Important to Measure Unbound Drug in Evaluating Nanomedicine Pharmacokinetics?," *Drug Metab Dispos*, vol. 44, no. 12, pp. 1934–1939, Dec. 2016, doi: 10.1124/dmd.116.073148.

[78] L. Van de Sande, S. Cosyns, W. Willaert, and W. Ceelen, "Albumin-based cancer therapeutics for intraperitoneal drug delivery: a review," *Drug Delivery*, vol. 27, no. 1, pp. 40–53, Jan. 2020, doi: 10.1080/10717544.2019.1704945.

[79] "Platinum Compounds: a New Class of Potent Antitumour Agents".

[80] A. Bonetti, R. Leone, F. M. Muggia, and S. B. Howell, Eds., *Platinum and Other Heavy Metal Compounds in Cancer Chemotherapy: Molecular Mechanisms and Clinical Applications*. Totowa, NJ: Humana Press, 2009. doi: 10.1007/978-1-60327-459-3.

[81] C. Zhang, C. Xu, X. Gao, and Q. Yao, "Platinum-based drugs for cancer therapy and anti-tumor strategies," *Theranostics*, vol. 12, no. 5, pp. 2115–2132, 2022, doi: 10.7150/thno.69424.

[82] N. Muhammad and Z. Guo, "Metal-based anticancer chemotherapeutic agents," *Current Opinion in Chemical Biology*, vol. 19, pp. 144–153, Apr. 2014, doi: 10.1016/j.cbpa.2014.02.003.

[83] C. Imberti, P. Zhang, H. Huang, and P. J. Sadler, "New Designs for Phototherapeutic Transition Metal Complexes," *Angew. Chem. Int. Ed.*, vol. 59, no. 1, pp. 61–73, Jan. 2020, doi: 10.1002/anie.201905171.

[84] K. Marković, R. Milačič, S. Marković, J. Kladnik, I. Turel, and J. Ščančar, "Binding Kinetics of Ruthenium Pyrithione Chemotherapeutic Candidates to Human Serum Proteins Studied by HPLC-ICP-MS," *Molecules*, vol. 25, no. 7, p. 1512, Mar. 2020, doi: 10.3390/molecules25071512.

[85] J. Coverdale, T. Laroiya-McCarron, and I. Romero-Canelón, "Designing Ruthenium Anticancer Drugs: What Have We Learnt from the Key Drug Candidates?," *Inorganics*, vol. 7, no. 3, p. 31, Mar. 2019, doi: 10.3390/inorganics7030031.

[86] J. Kljun *et al.*, "Pyrithione-based ruthenium complexes as inhibitors of aldo–keto reductase 1C enzymes and anticancer agents," *Dalton Trans.*, vol. 45, no. 29, pp. 11791–11800, 2016, doi: 10.1039/C6DT00668J.

[87] S. Ristovski, M. Uzelac, J. Kljun, T. Lipec, and M. Urs̆ic̆, "Organoruthenium Prodrugs as a New Class of Cholinesterase and Glutathione-S-Transferase Inhibitors," p. 11, 2018.

[88] K. Marković, M. Cemazar, G. Sersa, R. Milačič, and J. Ščančar, "Speciation of copper in human serum using conjoint liquid chromatography on short-bed monolithic disks with UV and post column ID-ICP-MS detection," *J. Anal. At. Spectrom.*, p. 10.1039.D2JA00161F, 2022, doi: 10.1039/D2JA00161F.

[89] B. R. Stern, "Essentiality and Toxicity in Copper Health Risk Assessment: Overview, Update and Regulatory Considerations," *Journal of Toxicology and Environmental Health, Part A*, vol. 73, no. 2–3, pp. 114–127, Jan. 2010, doi: 10.1080/15287390903337100.

[90] A. A. Taylor *et al.*, "Critical Review of Exposure and Effects: Implications for Setting Regulatory Health Criteria for Ingested Copper," *Environmental Management*, vol. 65, no. 1, pp. 131–159, Jan. 2020, doi: 10.1007/s00267-019-01234-y.

[91] A. Kubala-Kukuś *et al.*, "Analysis of Copper Concentration in Human Serum by Application of Total Reflection X-ray Fluorescence Method," *Biol Trace Elem Res*, vol. 158, no. 1, pp. 22–28, Apr. 2014, doi: 10.1007/s12011-013-9884-4.

[92] T. Kirsipuu *et al.*, "Copper(II)-binding equilibria in human blood," *Sci Rep*, vol. 10, no. 1, p. 5686, Dec. 2020, doi: 10.1038/s41598-020-62560-4.

[93] S. Cherukuri, R. Potla, J. Sarkar, S. Nurko, Z. L. Harris, and P. L. Fox, "Unexpected role of ceruloplasmin in intestinal iron absorption," *Cell Metabolism*, vol. 2, no. 5, pp. 309–319, Nov. 2005, doi: 10.1016/j.cmet.2005.10.003.

[94] N. E. Hellman, "CERULOPLASMIN METABOLISM AND FUNCTION," p. 20, 2002.

[95] D. Galaris, A. Barbouti, and K. Pantopoulos, "Iron homeostasis and oxidative stress: An intimate relationship," *Biochimica et Biophysica Acta (BBA) - Molecular Cell Research*, vol. 1866, no. 12, p. 118535, Dec. 2019, doi: 10.1016/j.bbamcr.2019.118535.

[96] AnnaL. P. Chapman *et al.*, "Ceruloplasmin Is an Endogenous Inhibitor of Myeloperoxidase," *Journal of Biological Chemistry*, vol. 288, no. 9, pp. 6465–6477, Mar. 2013, doi: 10.1074/jbc.M112.418970.

[97] A. V. Sokolov, V. A. Kostevich, E. T. Zakharova, V. R. Samygina, O. M. Panasenko, and V. B. Vasilyev, "Interaction of ceruloplasmin with eosinophil peroxidase as compared to its interplay with myeloperoxidase: Reciprocal effect on enzymatic properties," *Free Radical Research*, vol. 49, no. 6, pp. 800–811, Jun. 2015, doi: 10.3109/10715762.2015.1005615.

[98] I. Bento, C. Peixoto, V. N. Zaitsev, and P. F. Lindley, "Ceruloplasmin revisited: structural and functional roles of various metal cation-binding sites," p. 9, 2007.

[99] I. Matsuda, T. Pearson, and N. A. Holtzman, "Determination of Apoceruloplasmin by Radioimmunoassay in Nutritional Copper Deficiency, Menkes' Kinky Hair Syndrome, Wilson's Disease, and Umbilical Cord Blood," *Pediatr Res*, vol. 8, no. 10, pp. 821–824, Oct. 1974, doi: 10.1203/00006450-197410000-00001.

[100] B. Witt, D. Schaumlöffel, and T. Schwerdtle, "Subcellular Localization of Copper—Cellular Bioimaging with Focus on Neurological Disorders," *IJMS*, vol. 21, no. 7, p. 2341, Mar. 2020, doi: 10.3390/ijms21072341.

[101] G. Marchi, F. Busti, A. Lira Zidanes, A. Castagna, and D. Girelli, "Aceruloplasminemia: A Severe Neurodegenerative Disorder Deserving an Early Diagnosis," *Front. Neurosci.*, vol. 13, p. 325, Apr. 2019, doi: 10.3389/fnins.2019.00325.

[102] B. Wang and X.-P. Wang, "Does Ceruloplasmin Defend Against Neurodegenerative Diseases?," *CN*, vol. 17, no. 6, pp. 539–549, May 2019, doi: 10.2174/1570159X16666180508113025.

[103] V. Vassiliev, Z. L. Harris, and P. Zatta, "Ceruloplasmin in neurodegenerative diseases," *Brain Research Reviews*, vol. 49, no. 3, pp. 633–640, Nov. 2005, doi: 10.1016/j.brainresrev.2005.03.003.

[104] P. Smpokou, M. Samanta, G. T. Berry, L. Hecht, E. C. Engle, and U. Lichter-Konecki, "Menkes disease in affected females: The clinical disease spectrum," *Am. J. Med. Genet.*, vol. 167, no. 2, pp. 417–420, Feb. 2015, doi: 10.1002/ajmg.a.36853.

[105] S. H. Hahn, "Population screening for Wilson's disease: Population screening for Wilson's disease," *Ann. N.Y. Acad. Sci.*, vol. 1315, no. 1, pp. 64–69, May 2014, doi: 10.1111/nyas.12423.

[106] W. Lv *et al.*, "Noninvasive Prenatal Testing for Wilson Disease by Use of Circulating Single-Molecule Amplification and Resequencing Technology (cSMART)," *Clinical Chemistry*, vol. 61, no. 1, pp. 172–181, Jan. 2015, doi: 10.1373/clinchem.2014.229328.

[107] G. Grolez *et al.*, "Ceruloplasmin activity and iron chelation treatment of patients with Parkinson's disease," *BMC Neurol*, vol. 15, no. 1, p. 74, Dec. 2015, doi: 10.1186/s12883-015-0331-3.

[108] G. J. Brewer, S. H. Kanzer, E. A. Zimmerman, D. F. Celmins, S. M. Heckman, and R. Dick, "Copper and Ceruloplasmin Abnormalities in Alzheimer's Disease," *Am J Alzheimers Dis Other Demen*, vol. 25, no. 6, pp. 490–497, Sep. 2010, doi: 10.1177/1533317510375083.

[109] M. O. Louro, J. A. Cocho, A. Mera, and J. C. Tutor, "Immunochemical and enzymatic study of ceruloplasmin in rheumatoid arthritis," *Journal of Trace Elements in Medicine and Biology*, vol. 14, no. 3, pp. 174–178, Oct. 2000, doi: 10.1016/S0946-672X(00)80007-3.

[110] V. Tisato *et al.*, "TRAIL and Ceruloplasmin Inverse Correlation as a Representative Crosstalk between Inflammation and Oxidative Stress," *Mediators of Inflammation*, vol. 2018, pp. 1–8, Jul. 2018, doi: 10.1155/2018/9629537.

[111] R. Squitti *et al.*, "Serum copper profile in patients with type 1 diabetes in comparison to other metals," *Journal of Trace Elements in Medicine and Biology*, vol. 56, pp. 156–161, Dec. 2019, doi: 10.1016/j.jtemb.2019.08.011.

[112] D.-W. Zeng *et al.*, "Serum Ceruloplasmin Levels Correlate Negatively with Liver Fibrosis in Males with Chronic Hepatitis B: A New Noninvasive Model for Predicting Liver Fibrosis in HBV-Related Liver Disease," *PLoS ONE*, vol. 8, no. 10, p. e77942, Oct. 2013, doi: 10.1371/journal.pone.0077942.

[113] F. Chen *et al.*, "Ceruloplasmin correlates with immune infiltration and serves as a prognostic biomarker in breast cancer," *Aging*, vol. 13, no. 16, pp. 20438–20467, Aug. 2021, doi: 10.18632/aging.203427.

[114] Y. Mukae *et al.*, "Ceruloplasmin Levels in Cancer Tissues and Urine Are Significant Biomarkers of Pathological Features and Outcome in Bladder Cancer," *Anticancer Res*, vol. 41, no. 8, pp. 3815–3823, Aug. 2021, doi: 10.21873/anticanres.15174.

[115] I. W. Han *et al.*, "Ceruloplasmin as a prognostic marker in patients with bile duct cancer," *Oncotarget*, vol. 8, no. 17, pp. 29028–29037, Apr. 2017, doi: 10.18632/oncotarget.15995.

[116] M. Sogabe *et al.*, "Novel Glycobiomarker for Ovarian Cancer That Detects Clear Cell Carcinoma," *J. Proteome Res.*, vol. 13, no. 3, pp. 1624–1635, Mar. 2014, doi: 10.1021/pr401109n.

[117] R. Matsuoka *et al.*, "Heterotopic production of ceruloplasmin by lung adenocarcinoma is significantly correlated with prognosis," *Lung Cancer*, vol. 118, pp. 97–104, Apr. 2018, doi: 10.1016/j.lungcan.2018.01.012.

[118] D. A. da Silva *et al.*, "Copper in tumors and the use of copper-based compounds in cancer treatment," *Journal of Inorganic Biochemistry*, vol. 226, p. 111634, Jan. 2022, doi: 10.1016/j.jinorgbio.2021.111634.

[119] A. McNeill, M. Pandolfo, J. Kuhn, H. Shang, and H. Miyajima, "The Neurological Presentation of Ceruloplasmin Gene Mutations," *Eur Neurol*, vol. 60, no. 4, pp. 200–205, 2008, doi: 10.1159/000148691.

[120] H. Miyajima, "Aceruloplasminemia, an iron metabolic disorder," *Neuropathology*, vol. 23, no. 4, pp. 345–350, Dec. 2003, doi: 10.1046/j.1440-1789.2003.00521.x.

[121] A. Piperno and M. Alessio, "Aceruloplasminemia: Waiting for an Efficient Therapy," *Front. Neurosci.*, vol. 12, p. 903, Dec. 2018, doi: 10.3389/fnins.2018.00903.

[122] A. N. Prasad and R. Ojha, "Menkes disease: what a multidisciplinary approach can do," *JMDH*, vol. Volume 9, pp. 371–385, Aug. 2016, doi: 10.2147/JMDH.S93454.

[123] M. T. Lorincz, "Neurologic Wilson's disease: Wilson's disease," *Annals of the New York Academy of Sciences*, vol. 1184, no. 1, pp. 173–187, Jan. 2010, doi: 10.1111/j.1749-6632.2009.05109.x.

[124] I. Infusino, C. Valente, A. Dolci, and M. Panteghini, "Standardization of ceruloplasmin measurements is still an issue despite the availability of a common reference material," *Anal Bioanal Chem*, vol. 397, no. 2, pp. 521–525, May 2010, doi: 10.1007/s00216-009-3248-0.

[125] E. Martínez-Morillo and J. M. Bauça, "Biochemical diagnosis of Wilson's disease: an update," *Advances in Laboratory Medicine / Avances en Medicina de Laboratorio*, vol. 3, no. 2, pp. 103–113, Jun. 2022, doi: 10.1515/almed-2022-0020.

[126] K. Inagaki *et al.*, "Speciation of protein-binding zinc and copper in human blood serum by chelating resin pre-treatment and inductively coupled plasma mass spectrometry," *Analyst*, vol. 125, no. 1, pp. 197–203, 2000, doi: 10.1039/a907088e.

[127] V. Lopez-Avila, O. Sharpe, and W. H. Robinson, "Determination of ceruloplasmin in human serum by SEC-ICPMS," *Anal Bioanal Chem*, vol. 386, no. 1, pp. 180–187, Aug. 2006, doi: 10.1007/s00216-006-0528-9.

[128] K. Kobayashi *et al.*, "Direct Analysis of Ceruloplasmin in Human Blood Serum by HPLC/Inductively Coupled Plasma-Mass Spectrometry for the Diagnosis of Wilson Disease," p. 5.

[129] B. Bernevic, A. H. El-Khatib, N. Jakubowski, and M. G. Weller, "Online immunocapture ICP-MS for the determination of the metalloprotein ceruloplasmin in human serum," *BMC Res Notes*, vol. 11, no. 1, p. 213, Dec. 2018, doi: 10.1186/s13104-018-3324-7.

[130] C. D. Quarles *et al.*, "LC-ICP-MS method for the determination of 'extractable copper' in serum," *Metallomics*, vol. 12, no. 9, pp. 1348–1355, Sep. 2020, doi: 10.1039/d0mt00132e.

[131] M. Costas-Rodríguez, Y. Anoshkina, S. Lauwens, H. Van Vlierberghe, J. Delanghe, and F. Vanhaecke, "Isotopic analysis of Cu in blood serum by multi-collector ICP-mass spectrometry: a new approach for the diagnosis and prognosis of liver cirrhosis?," *Metallomics*, vol. 7, no. 3, pp. 491–498, 2015, doi: 10.1039/C4MT00319E.

[132] M. Aramendía, L. Rello, M. Resano, and F. Vanhaecke, "Isotopic analysis of Cu in serum samples for diagnosis of Wilson's disease: a pilot study," *J. Anal. At. Spectrom.*, vol. 28, no. 5, p. 675, 2013, doi: 10.1039/c3ja30349g.

[133] K. Hobin, M. Costas-Rodríguez, E. V. Wonterghem, R. E. Vandenbroucke, and F. Vanhaecke, "High-Precision Isotopic Analysis of Cu and Fe via Multi-Collector Inductively Coupled Plasma-Mass Spectrometry Reveals Lipopolysaccharide-Induced Inflammatory Effects in Blood Plasma and Brain Tissues," *Frontiers in Chemistry*, vol. 10, p. 10, 2022.

[134] S. Wilschefski and M. Baxter, "Inductively Coupled Plasma Mass Spectrometry: Introduction to Analytical Aspects," *CBR*, vol. 40, no. 3, pp. 115–133, Aug. 2019, doi: 10.33176/AACB-19-00024.

[135] J. Vogl, "Characterisation of reference materials by isotope dilution mass spectrometry," *J. Anal. At. Spectrom.*, vol. 22, no. 5, p. 475, 2007, doi: 10.1039/b614612k.

[136] P. Rodríguez-González, J. M. Marchante-Gayón, J. I. García Alonso, and A. Sanz-Medel, "Isotope dilution analysis for elemental speciation: a tutorial review," *Spectrochimica Acta Part B: Atomic Spectroscopy*, vol. 60, no. 2, pp. 151–207, Feb. 2005, doi: 10.1016/j.sab.2005.01.005.

[137] T. W. May and R. H. Wiedmeyer, "A Table of Polyatomic Interferences in ICP-MS," *Atomic Spectroscopy*, vol. 19 (5), Sep. 1998, [Online]. Available: https://resources.perkinelmer.com/corporate/cmsresources/images/44-74379atl_tableofpolyatomicinterferences.pdf

[138] D. Sleep, "Albumin and its application in drug delivery," *Expert Opinion on Drug Delivery*, vol. 12, no. 5, pp. 793–812, May 2015, doi: 10.1517/17425247.2015.993313.

[139] F. Yang, Y. Zhang, and H. Liang, "Interactive Association of Drugs Binding to Human Serum Albumin," *IJMS*, vol. 15, no. 3, pp. 3580–3595, Feb. 2014, doi: 10.3390/ijms15033580.

[140] S. Seršen *et al.*, "Structure-Related Mode-of-Action Differences of Anticancer Organoruthenium Complexes with β-Diketonates," *J. Med. Chem.*, vol. 58, no. 9, pp. 3984–3996, May 2015, doi: 10.1021/acs.jmedchem.5b00288.

[141] Y. Sheng *et al.*, "Covalent versus Noncovalent Binding of Ruthenium η^6 - *p* - Cymene Complexes to Zinc-Finger Protein NCp7," *Chem. Eur. J.*, vol. 25, no. 55, pp. 12789–12794, Oct. 2019, doi: 10.1002/chem.201902434.

[142] J. Nagaj, K. Stokowa-Sołtys, E. Kurowska, T. Frączyk, M. Jeżowska-Bojczuk, and W. Bal, "Revised Coordination Model and Stability Constants of Cu(II) Complexes of Tris Buffer," *Inorg. Chem.*, vol. 52, no. 24, pp. 13927–13933, Dec. 2013, doi: 10.1021/ic401451s.

[143] H. E. Mash, Y.-P. Chin, L. Sigg, R. Hari, and H. Xue, "Complexation of Copper by Zwitterionic Aminosulfonic (Good) Buffers," *Anal. Chem.*, vol. 75, no. 3, pp. 671–677, Feb. 2003, doi: 10.1021/ac0261101.

[144] J. A. Schmidt *et al.*, "Plasma concentrations and intakes of amino acids in male meat-eaters, fish-eaters, vegetarians and vegans: a cross-sectional analysis in the EPIC-Oxford cohort," *Eur J Clin Nutr*, vol. 70, no. 3, pp. 306–312, Mar. 2016, doi: 10.1038/ejcn.2015.144.

[145] J. Healy and K. Tipton, "Ceruloplasmin and what it might do," *J Neural Transm*, vol. 114, no. 6, pp. 777–781, Jun. 2007, doi: 10.1007/s00702-007-0687-7.

[146] P. Ravisankar, S. Anusha, K. Supriya, and U. A. Kumar, "Fundamental Chromatographic Parameters," no. 09, p. 5.

[147] S. Dasdelen and S.-O. Grebe, "Infections after renal transplantation," *LaboratoriumsMedizin*, vol. 41, no. 2, Jan. 2017, doi: 10.1515/labmed-2017-0094.

Bibliography

Publications Related to the Thesis

Journal Articles

Katarina Marković, Radmila Milačič, Stefan Marković, Jerneja Kladnik, Iztok Turel, Janez Ščančar, "Binding kinetics of ruthenium pyrithione chemotherapeutic candidates to human serum proteins studied by HPLC-ICP-MS", Molecules, 2020, vol. 25, no. 7, str. 1512-1-1512-13, ISSN 1420-3049, DOI: 10.3390/molecules25071512. [COBISS.SI-ID 33282855]

Katarina Marković, Maja Čemažar, Gregor Serša, Radmila Milačič, Janez Ščančar, "Speciation of copper in human serum using conjoint liquid chromatography on short-bed monolithic disks with UV and post column ID-ICP-MS detection", Journal of analytical atomic spectrometry, 2022, vol. 37, no. 8, str. 1675-1686, ISSN 0267-9477, DOI: 10.1039/D2JA00161F. [COBISS.SI-ID 113592835]

Conference Paper Related to the Thesis

Katarina Marković, Janja Vidmar, Stefan Marković, Iztok Turel, Jerneja Kladnik, Janez Ščančar, Radmila Milačič, "Speciation of Ruthenium-based complexesin human serum by conjoint liquid chromatography on monolithic columns", V: Knjiga povzetkov : science of the future how to stay up-to-date with your research! = Book of abstracts, 11. študentska konferenca Mednarodne podiplomske šole Jožefa Stefana in 13. dneva mladih raziskovalcev (Konferenca KMBO), 15. in 16. april 2019, Planica, Slovenija = 11th Jožef Stefan International Postgraduate School Students' Conference and 13th Young Researchers' Day, 15th and 16th May 2019, Planica, Slovenia, Martin Topole (ur.), et al., Ljubljana: Mednarodna podiplomska šola Jožefa Stefana: = Jožef Stefan International Postgraduate School: Inštitut Jožef Stefan: = Jožef Stefan Institute, 2019, str. 32, http://ipssc.mps.si/Proceedings/Proceedings2019.pdf. [COBISS.SI-ID 33145383]

Katarina Marković, Speciation of copper in human serum by conjoint liquid chromatography and inductively coupled plasma mass spectrometry - YRC : presented at 9th hibrid Monolit Summer Symposium, Portorož, June 13th-17th 2022. [COBISS.SI-ID 111811075]

Other Publications

Katarina Marković, Radmila Milačič, Janja Vidmar, Stefan Marković, Katja Uršič Valentinuzzi, Martina Nikšić Žakelj, Maja Čemažar, Gregor Serša, Mojca Unk, Janez Ščančar, "Monolithic chromatography on conjoint liquid chromatography columns for speciation of platinum-based chemotherapeutics in serum of cancer patients", Journal of trace elements in medicine and biology, 2020, vol. 57, str. 28-39, ISSN 0946-672X, DOI: 10.1016/j.jtemb.2019.09.011. [COBISS.SI-ID 32667175]

Xuan Xu, Sašo Šturm, Zoran Samardžija, Janez Ščančar, Katarina Marković, Kristina Žužek Rožman, "A facile method for the simultaneous recovery of rare-earth elements and transition metals from Nd-Fe-B magnets", Green chemistry, 2020, vol. 22, no. 5, str. 1105-1112, ISSN 1463-9262, DOI: 10.1039/c9gc03325d. [COBISS.SI-ID 33069351]

Dimitrija Savić Zdravković, Djuradj Milošević, Jelena Conić, Katarina Marković, Janez Ščančar, Marko Miliša, Boris Jovanović, "Revealing the effects of cerium dioxide nanoparticles through the analysis of morphological changes in Chironomus riparius", Science of the total environment, 2021, vol. 786, str. 147439-1-147439-14, ISSN 0048-9697, DOI: 10.1016/j.scitotenv.2021.147439. [COBISS.SI-ID 64844803]

Guanglong Ma, Nina Kostevšek, Boštjan Markelc, Samo Hudoklin, Mateja Erdani-Kreft, Igor Serša, Maja Čemažar, Katarina Marković, Janez Ščančar, et al., "PD1 blockade potentiates the therapeutic efficacy of photothermally-activated and MRI-guided low temperature-sensitive magnetoliposomes", Journal of controlled release, [Print ed.], 2021, vol. 332, str. 419-433, ilustr., ISSN 0168-3659, DOI: 10.1016/j.jconrel.2021.03.002. [COBISS.SI-ID 54376707]

Stefanie Nübler, Stefan Marković, Katarina Marković, et al., "Interlaboratory Comparison Investigations (ICIs) for human biomonitoring of chromium as part of the quality assurance programme under HBM4EU", Journal of trace elements in medicine and biology, [in press] 2022, vol. 70, str. 126912-1-126912-8, ISSN 0946-672X, DOI: 10.1016/j.jtemb.2021.126912. [COBISS.SI-ID 89702915]

Xuan Xu, Sina Khoshima, Milana Karajić, Jan Balderman, Katarina Marković, Janez Ščančar, Zoran Samardžija, Sašo Šturm, Kristina Žužek Rožman, "Electrochemical routes for environmentally friendly recycling of rare-earth-based (Sm–Co) permanent magnets", Journal of Applied Electrochemistry, 2022, vol. 52, iss. 4, str. 10, ilustr., ISSN 0021-891X, DOI: 10.1007/s10800-022-01696-9. [COBISS.SI-ID 103408899]

Biography

Katarina Marković was born on 11-01-1992 in Užice, Serbia. She finished gymnasium in 2011 in Požega and started (4-year) studies at the Faculty of Chemistry at Belgrade University in Environmental Chemistry. In 2016 she obtained a bachelor's degree. During her studies she had an internship (4 months) at the Water Supply Company in Belgrade as a part of a project organized by the Career Development Centre "Bg Praksa". She also worked on a faculty promotion campaign. In 2016/2017, she enrolled in a two-year second-level master's study programme at the University of Nova Gorica (UNG), School of Environmental Sciences and successfully completed the first year. During her studies at UNG she worked with assist. Prof. Dr. Suzana Žižek on studies of the aquatic toxicity of mercury, cadmium and copper to *Daphnia Magna*. In 2017/2018 she enrolled on the second year of the master's study of Ecotechnologies at the Jožef Stefan International Postgraduate School (IPS) under the supervision of Prof. Dr. Janez Ščančar. The experimental part of her master thesis was performed at the Department of Environmental Sciences (DES) of the Jožef Stefan Institute. Her research work was focused on the speciation of Pt-based chemotherapeutics in the human serum of cancer patients. She defended her master's degree in 2018. Then she continued with PhD studies at the IPS, in the doctoral study programme Ecotehnologies under the supervision of Prof. Dr. Radmila Milačič. Katarina was employed as a young researcher at the DES. During her PhD studies, Katarina worked for two months at the Institute of Water Quality and Resource Management at TU WIEN, guided by Dr. Ernis Saracevic and Univ. Prof. Dipl.-Ing. Dr. Matthias Zessner on optimizing a new analytical method for PFAS determination in river water, influent and effluent wastewater samples by LC-MS/MS within Danube Hazard m3c European project.

Katarina's research interest is focused on developing new analytical methods for trace-element speciation analysis in biological samples.